CHALMERS

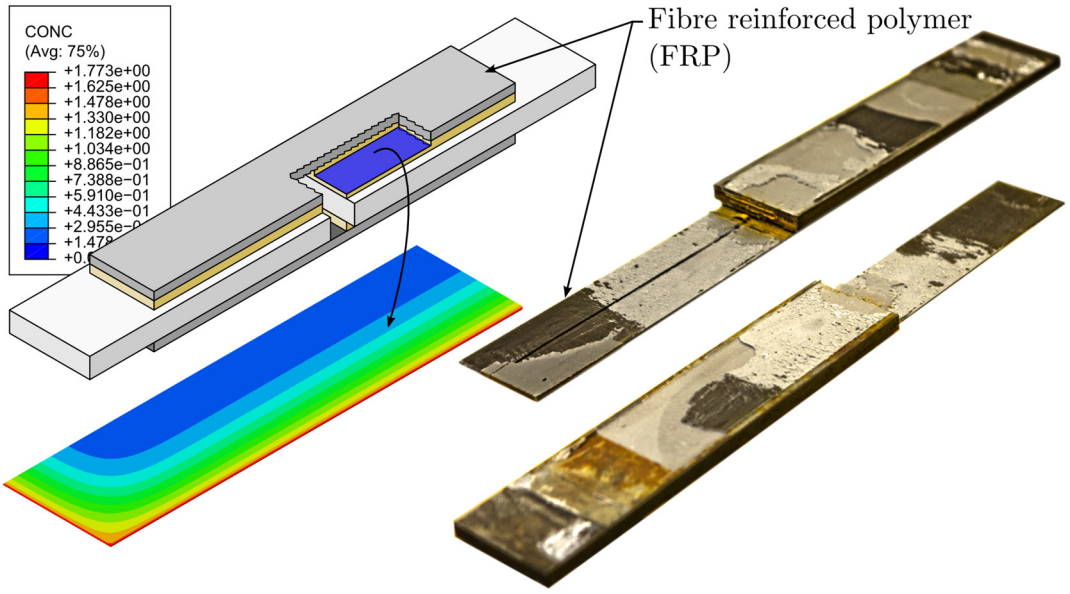

Hygrothermal Durability of Adhesively Bonded FRP/steel Joints

MOHSEN HESHMATI

Department of Civil and Environmental Engineering
Division of Structural Engineering
Steel and Timber Structures
CHALMERS UNIVERSITY OF TECHNOLOGY
Gothenburg, Sweden 2015

THESIS FOR THE DEGREE OF LICENTIATE OF ENGINEERING

Hygrothermal Durability of Adhesively Bonded FRP/Steel Joints

MOHSEN HESHMATI

Department of Civil and Environmental Engineering
Division of Structural Engineering
Steel and Timber Structures
CHALMERS UNIVERSITY OF TECHNOLOGY

Gothenburg, Sweden 2015

Hygrothermal Durability of Adhesively Bonded FRP/Steel Joints

MOHSEN HESHMATI

© MOHSEN HESHMATI, 2015

Thesis for the degree of Licentiate of Engineering 2015:02
ISSN no. 1652-9146
Department of Civil and Environmental Engineering
Division of Structural Engineering
Steel and Timber Structures
Chalmers University of Technology
SE-412 96 Gothenburg
Sweden
Telephone: + 46 (0)31-772 1000

Cover:
Left: simulated moisture profile in adhesive layer of an FRP/steel bonded joint, right: photograph of failed specimen tested after one year of immersion in water at 45°C. Photographed and created by the author.

Chalmers Reproservice
Gothenburg, Sweden, 2015

Hygrothermal Durability of Adhesively Bonded FRP/Steel Joints

MOHSEN HESHMATI
Department of Civil and Environmental Engineering
Division of Structural Engineering
Steel and Timber Structures
Chalmers University of Technology

Abstract

Fibre reinforced polymer (FRP) composites offer superior mechanical properties, such as specific strength and stiffness, corrosion resistance and light weight. Over the past four decades, FRPs have been increasingly used for strengthening and repair of bridge structures, and more recently, in the manufacture of whole/hybrid FRP bridges. In such applications, adhesive bonding is usually the preferred joining technique. Although, the short-term behaviour of FRP/steel bonded joints has been extensively studied, the subject of the durability has not been researched to the same degree. In addition, existing numerical and experimental approaches for the characterization of the durability of bonded FRP/steel joints have mainly been developed with reference to applications in the aerospace industry, where mechanical and environmental loads differ considerably compared with those in civil engineering applications. Today, uncertainties regarding the durability aspects of adhesively bonded FRP/steel joints used in bridges present a major obstacle to their growing application. There is, therefore, a clear need for research work which focuses on the durability and long-term performance of bonded FRP/steel joints used in bridges.

The lack of knowledge regarding the long-term performance is currently compensated by applying a multiple of large safety factors to the strength of composite materials, which dramatically increases the material usage and reduces the design efficiency. The aim of this research work is to shed some light on the durability and long-term performance of adhesively bonded FRP/steel joints with emphasis on effect of hygrothermal ageing on mechanical behaviour of such joints. To realize this aim, experimental, numerical and analytical approaches are used. The work includes long-term experiments on double lap shear joints with different adherends subjected to various temperature ranges, humidity levels, and cyclic exposure scenarios. Complementary material characterization tests are also conducted to study the moisture diffusion kinetics, and moisture dependent mechanical and fracture properties. The results are used as input in FE simulations to predict the moisture induced stress redistribution in the joints and the behaviour of the joints up to failure.

The test results of hygrothermally aged joints indicate a clear change of failure mode from cohesive to interfacial or interlaminar failure. Even though all the joints exhibited increasing load-bearing capacity during the first six months, the failure load of specimens aged at higher temperatures started to degrade afterwards. Cohesive zone modelling approach was capable of accurately predicting the behaviour of the studied FRP/steel joints with different failure modes. The Fickian diffusion was found to yield accurate predictions for all tested materials. Moreover, the 3D moisture diffusion in orthotropic FRP composites was characterized and successfully modelled using FE mass diffusion analysis. The permeability of adherends was found to significantly affect moisture ingression into the joints. The joint level experiments in combination with the coupled mass diffusion-mechanical analysis indicated the existence of a critical period after which the strength degradation is likely to occur.

Keywords: Fibre reinforced polymer, durability, long-term performance, adhesively bonded FRP/steel joints, moisture diffusion, cohesive zone modelling

To Parisa

Preface

The work presented in this licentiate thesis explores the hygrothermal durability of adhesively bonded FRP/steel joints used in bridge applications. The project was carried out at the Department of Civil and Environmental Engineering, Division of Structural Engineering, Steel and Timber Structures, Chalmers University of Technology from June 2012 until January 2015. The author wishes to express his gratitude to the Swedish Research Institute, *FORMAS*, for financing this project.

I would like express my sincere gratitude to my supervisors, Prof. Mohammad Al-Emrani and Asst. Prof. Reza Haghani, for the trust they put in me, and also their encouragement, advice and valuable discussions throughout the study. Mohammad, it has been my privilege to work closely with you. I have enjoyed the opportunity to watch and learn from your knowledge and experience. Reza, you have been a tremendous mentor for me. I would like to thank you for encouraging my research and for allowing me to grow as a research scientist. I would also like to thank my examiner Prof. Robert Kliger for all his good advice and continuous support. I also appreciate the co-operation with Alan André, PhD. Special thanks go to Mrs. Jeanette Kliger for reading and improving my papers.

In my daily work I have been blessed with a friendly and cheerful group of colleagues at the Division of Structural Engineering. I would like to thank all my colleagues for their interest in my project and for stimulating discussions. Special thanks go to Thomas Lechner, my office mate for several months. We had plenty of talks and critical discussions which I will always remind and appreciate. I would like to thank my very good friend Mohammad Tahershamsi for his friendship, guidance, help and suggestions. I want to thank, as well, Farshid for his helpful discussions, and Poja for helping me to improve my Swedish. I am also grateful to the technical staff at Chalmers, Lars Wahlström, Marek Machowski and Sebastian Almfeldt, for their help and excellent work during the execution of tests.

I offer my most sincere thanks to my family, specially my parents whose everlasting support and encouragement provided me valuable motivation. This work couldn't have been done without patience and unconditional support and love from my wife, Parisa, whom I am deeply grateful to. Her encouragement, quiet patience and unwavering love were undeniably the bedrock upon which the past few years of my life have been built.

Gothenburg, 2015

Mohsen Heshmati

List of publications

This thesis is based on the work contained in the following papers:

Paper I

Heshmati M., Haghani R. and Al-Emrani M. (2014): Environmental Durability of Adhesively Bonded FRP/steel Joints in Civil Engineering Applications: State-of-the-Art. Submitted for publication to *Journal of Construction and Building Materials.*

Paper II

Heshmati M., Haghani R. André A. and Al-Emrani M. (2014): Experimental Characterisation and Numerical Modelling of the Interfacial and Cohesive Failure in FRP/steel Joints Bonded with Thick Adhesive Layer. Submitted for publication to *Journal of Construction and Building Materials.*

Paper III

Heshmati M., Haghani R. and Al-Emrani M. (2015): Effects of Moisture on the Long-term Performance of Adhesively Bonded FRP/steel Joints in Bridges – an Experimental and Numerical study. Submitted for publication to *Journal of Composite Structures.*

Author's contributions to jointly published papers

The contribution of the author of this licentiate thesis to the appended papers is described here.

I. Responsible for the writing and planning of the paper.

II. Responsible for the writing and for the major part of the planning of the paper. Planned the major part and was partly responsible for the execution of the experiments.

III. Responsible for the writing and planning of the paper. Responsible for planning and the execution of the experiments.

Additional publications by the author

Journal Papers

Aygül, M., Bokesjö, M., Heshmati, M., & Al-Emrani, M. (2013): A comparative study of different fatigue failure assessments of welded bridge details. *International Journal of Fatigue*,2013, 49, 62-72.

Haghani, R., Al-Emrani, M., & Heshmati, M. (2012): Fatigue-prone details in steel bridges. *Buildings*, 2014, 2(4), 456-476.

Conference Papers

Heshmati M., Haghani R. André A. and Al-Emrani M. (2014): Design of FRP/steel joints bonded with thick adhesive layers. *Proc. of the Second Intl. Conf. on Advances in Civil and Structural Engineering - CSE 2014*, Kuala Lumpur, Malaysia, 20-21 December 2014.

Heshmati, M., Al-Emrani, M. (2012): Fatigue design of plated structures using structural hot spot stress approach. *Proceedings of the Sixth International Conference on Bridge Maintenance, Safety and Management - IABMAS 2012*, Stresa, Lake Maggiore, 8-12 July 2012. p. 3146-3153. ISBN 978-041562124-3.

Heshmati, M., Al-Emrani, M. and Edlund B. (2012): Fatigue assessment of weld terminations in welded cover-plate details; A comparison of local approaches. *Nordic Steel Construction Conference*, Oslo, Sept 5-7, 2012. p. 781-790. ISBN 978-82-91466-12-5.

Master's Thesis

Heshmati, M. (2012): Fatigue life assessment of bridge details using finite element method. *Master's thesis*, Chalmers University of Technology, 2012:3.

Contents

Extended Summary

1 Introduction

1.1 Background

The design life of many civil engineering structures is 50-100 years, yet of many bridges that were built in different parts of the world before the middle of the last century, the majority are still in service. According to a recent study [1], steel bridges account for a large stock of old European bridges that have reached or will soon reach the end of their service-life. As opposed to rebuilding these bridges, strengthening and retrofitting could be a more economical solution provided that conventional repair methods are replaced by more durable and cost-effective upgrading techniques [2].

Fibre reinforced polymer (FRP) composites were firstly introduced in aerospace industry during 1940s. Despite superior properties of FRPs in structural applications, high production costs initially prevented their acceptance in extremely cost-driven and conservative construction industry. Nevertheless, continues growth of FRP industry lowered production costs, and FRP materials finally found their acceptance in construction industry during the late 1980s [3]. FRPs offer superior advantages over conventional construction materials such as steel, the most notable of which are their corrosion resistance, high strength-to-weight ratio and light weight. With the advances in polymer science, adhesive bonding has become a prominent joining technology that possesses several advantages over mechanical fastening techniques, such as lower weight, less fabrication costs and more uniform stress distribution. The unique properties of FRP composites combined with advantages of adhesive bonding, has made FRP bonding an attractive method for strengthening, repair and refurbishment of existing structures.

In the past four decades, Carbon fibre-reinforced polymer, CFRP, laminates have been used in practice to strengthen and repair concrete structures [4]. In the past few years, there has been also a trend towards the use of FRP bonding technique to strengthen and repair of steel [5,6] and timber structures [7,8]. Moreover, FRP materials have found their way into whole- and partial-FRP structures, e.g. using FRP deck systems on steel girders for the construction of hybrid FRP bridges or the refurbishment of existing steel bridges. As a result, there is a great deal of interest in studying the behaviour of FRP/steel adhesive joints from the short- and long-term behaviour perspectives.

One problem with application of FRP/steel joints in construction industry is uncertainties regarding the long-term performance of such joints. As in many other structures exposed

to outdoor environments, the effectiveness and success of adhesively-bonded FRP/steel joints in bridges is dependent on environmental durability of each and every constituent. In spite of the fact that existing FRP joints in bridges have exhibited acceptable outdoor performance with very seldom problems being reported in the literature, their relatively new application and lack of knowledge regarding their long-term performance and environmental degradation mechanisms have hindered their widespread application in steel structures. This lack of knowledge is currently compensated by applying a multiple of large safety factors to the strength of composite materials, which dramatically increases the material usage [5,9].

Concerns relating to the environmental durability of adhesive joints have manifested itself in recent research publications, in which understanding the underlying mechanisms of degradation [10–12] and quantifying the long-term performance [13,14] have been in focus. However, most of these research projects have been conducted within fields such as aerospace and automobile industry that have distinct differences with civil engineering applications [15,16]. Loading type, curing conditions, operating environments, material production, joint geometry, and manufacturing conditions are some examples of the aforementioned dissimilarities. In fact, there is still a lack of knowledge about the long-term performance of different adhesives and FRP composites (i.e. on material level) used in infrastructural applications.

A common approach to investigate the long-term performance issues is to use accelerated testing scenarios. In such tests, usually very harsh cyclic scenarios are formulated to achieve high damage rate in a relatively short time. Nevertheless, due to the unrealistically severe applied conditions, these tests tend to exaggerate the degradation rate. Furthermore, the use of accelerating parameters such as high temperature, may activate damaging mechanisms that may never happen during the life cycle of bridges. Hence, while the use of such conditions may be justifiable for automotive and aerospace industries, their validity for bridges and similar structures, with a much longer service life and less harsh exposure conditions, is doubtful. Another shortcoming of accelerated tests is the lack of time correlation between the test and real service conditions, which makes it almost impossible to accurately predict the service life of bridges.

With the improved computational capabilities in recent years, numerical methods have provided new possibilities to investigate complex issues such as the long-term performance more effectively. However, the results obtained from these methods need to be correlated and verified by observations and/or testing of structures in real conditions before they can be considered reliable. In addition, given the uncertainties regarding the long-term behaviour of bonded FRP joints in bridge structures, modelling the possible synergies between various damaging mechanisms becomes inherently cumbersome. Therefore, there is a strong need to develop accurate durability data and experimentally verified assessment approaches valid for adhesively bonded FRP/steel joints used in bridge applications.

1.2 Aim and objectives

The overall aim of the project is to establish a framework for the long-term performance and durability assessment of adhesively bonded FRP/steel joints exposed to any combination of moisture and temperature (hygrothermal ageing). Within this overall aim, the following main objectives are defined and covered in this thesis:

- To review the state-of-the-art on durability of FRP composites, structural adhesives and FRP/steel bonded joints used in bridge applications with the emphasis on identifying the influential environmental factors, damaging mechanisms, and collecting the available long-term performance data.
- To study the behaviour of FRP/steel joints bonded with thick adhesive layer using advanced numerical approaches such as the damage mechanics approach.
- To characterize the temperature and moisture dependent material properties and implement the outcome in the developed modelling basis.
- To investigate how hygrothermal conditions affect the performance of adhesively bonded FRP/steel joints.

Additional objectives that are not addressed in this thesis and will be investigated in the continuation of this project are:

- To characterize the moisture, history (cyclic exposure) and combined moisture-temperature dependent fracture properties of adhesive, adhesive/steel interface, and FRP bonded joints.
- To investigate, characterize and predict the effect of sub-zero exposure conditions on mechanical properties of adhesively bonded joints
- To predict the residual strength and behaviour of environmentally aged bonded joints exposed to hygrothermal conditions.

1.3 Method and scientific approach

Figure 1.1 shows the methodology that has been used to realize the overall aim of this project. As can be seen, the methodology is divided into two phases. It was intended to address the objectives of this thesis during the first phase, whereas the additional objectives will be addressed in the continuation of the project and during the second phase.

In this context, both experimental and numerical tools were used. An extensive literature study was performed to obtain the state-of-the-art on durability of adhesively bonded FRP/steel joints used in civil engineering applications. Special consideration was given to

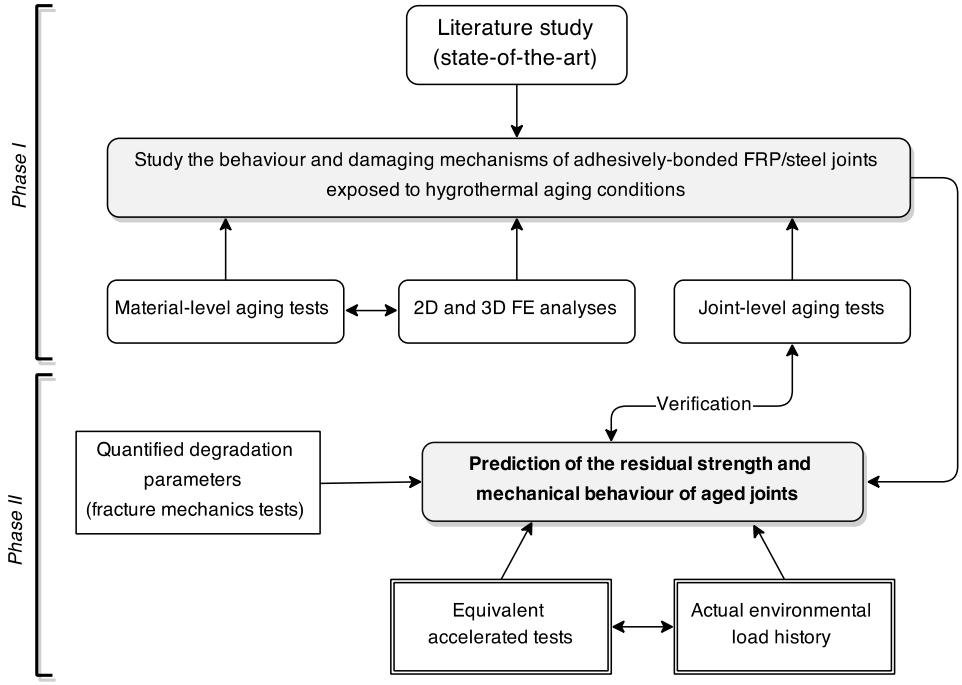

Figure 1.1. *Method for the study.*

identifying the common long-term performance assessment approaches, possible synergies between various ageing factors, and the relevant experimental results.

Based on the findings of the literature study, a series of experiments were designed to characterize the effect of hygrothermal ageing conditions on material and joint-level. Given that the aim of the project is to establish a methodology that can be applicable to any types of composites, adhesives, steel, etc., no attempt is made to compare different types of materials. Hence, only one type of each material is used in the experimental work. Furthermore, the applicability of the cohesive zone modelling concept to predict the strength of bonded FRP/steel joints, with interfacial and/or cohesive failure modes, was investigated by means of 2D finite element (FE) analyses. In addition, coupled 3D FE analyses were performed to study the effects of moisture on the mechanical response of bonded FRP/steel joints.

1.4 Limitations

The work in this thesis involved studying the hygrothermal durability of adhesively bonded FRP/steel joints. The following limitations apply in this thesis:

(1) Only one type of adhesive, steel, CFRP, and GFRP materials were considered, and therefore the results might not be applicable to other materials.
(2) Only temperatures below the glass transition temperature of adhesive and above the room temperature were utilized.

(3) Only quasi-static loads were considered.
(4) The interfacial moisture diffusion, creep and load-assisted diffusion were neglected in the mass diffusion finite element analyses.
(5) Possible size-effects were not included.
(6) Due to the time limitation, only some of the test results are presented in this thesis. However, the described experiments are ongoing and further results are expected to be obtained in the future.

1.5 Outline of the thesis

This thesis consists of an introductory section and three main papers.

Chapter 2 introduces the durability of adhesively bonded FRP/steel joints in the presence of moisture by reporting the effects of moisture on FRP composites and epoxy adhesives. This knowledge is extended through Paper I which presents a review on hygrothermal durability of adhesively bonded FRP/steel joints.

Chapter 3 provides an overview of the experimental programme as well as the materials. Different tests and environmental conditions are described

Chapter 4 presents a detailed description of the tests aimed at material characterization. The results of the completed tests are presented and discussed. In addition, the planned tests are described.

Chapter 5 introduces the long-term performance tests using double lap shear joints. The configuration of specimens, fabrication procedures, and exposure scenarios are described. Moreover, the test results on joints with CFRP adherend are presented and the findings are discussed.

Chapter 6 provides an overview of the modelling scheme. The purpose of the used numerical modelling approaches as well as their relation to the rest of the study are explained.

Chapter 7 and Paper II present the established characterization and modelling approach used to predict the strength and behaviour of bonded FRP/steel joints with thick adhesive layer.

Chapter 8 and Paper III present the results of coupled finite element analyses used to study the effects of moisture on performance of adhesively bonded FRP/steel joints.

In chapter 9, the main conclusions from this work are drawn and suggestions for the future work are given.

2 Durability of adhesively bonded FRP/steel joints in the presence of moisture

2.1 Introduction

Moisture is one of the most problematic substances when discussing environmental durability of adhesive joints with metallic adherend(s) [11]. Many civil engineering structures will inevitably be in direct contact with moisture during their lifetime. This is either due to the design considerations or location, or due to accidental or natural causes. Moisture, either as vapour, liquid water or de-icing salt solutions, can penetrate into adhesively bonded joints by diffusion through the adhesive layer, or wicking along the interfaces, or absorption through the porous adherend [17]. The penetrated moisture can affect joint mechanical properties through two principal mechanisms; (i) degradation of adhesive and/or adherends; (ii) degradation of adherend/adhesive interface(s) [18–21].

Depending on the polymer structure and chemical composition, the absorbed moisture can affect adhesive or FRP material properties in a reversible manner, such as plasticization, or in an irreversible manner, such as chemical or physical breakdown of bonds. However, as will be discussed later, low concentrations of water and subsequently a small amount of moisture-induced plasticization may actually be beneficial in some joints as studied in [22]. The absorbed moisture, can also attack the interface either by displacing the adhesive or hydrating the metal or metal oxide [19,22]. Despite the debasing effects of moisture on the strength of adhesive joints, there are indications of a critical relative humidity in the surrounding air below which the weakening does not occur [23].

Moisture triggers different ageing mechanisms for each component of adhesively bonded FRP/steel joints. Therefore, in this section, the effects of moisture on FRP composts as the adherend, epoxy adhesive as the most frequent bonding material in construction sector, and eventually the overall FRP/steel bonded joint is discussed.

2.2 Effect of moisture on FRP composites

FRPs, like all organic polymers, are susceptible to moisture diffusion which can alter their thermo-physical, mechanical, and chemical characteristics. The ageing mechanisms of FRP composites in aqueous environments involve both chemical and physical aspects. Physical degradation, which is basically temperature dependent, may dramatically change material properties. However, these changes are reversible and will be recovered upon drying. Chemical degradation is accompanied by irreversible material alteration in every constituent level, and is usually initiated upon longer exposure durations or harsher conditions. Moisture can potentially attack FRP composites by one or a combination of the following mechanisms: (i) altering resin matrix; (ii) damaging fibre/matrix interface; (iii) fibre-level degradation.

2.2.1 Effect of moisture on resin matrix

Moisture primarily affects the resin matrix. Various mechanisms of degradation for different types of resins, such as epoxy, polyester and vinyl-ester, are well documented. In general, moisture can alter resin by plasticization, swelling, cracking, hydrolysis, and fibre/matrix debonding [24–26]. Zhou and Lucas [27] studied the interaction of water molecules with epoxy resins. The study showed that depending on the required activation energy for desorption, two types of bound water can be found in epoxy resins; Type I or Type II. Type I bound water is manifested by disrupting the weaker inter-chain Van der Waals forces and acts as plasticizer. On the other hand, Type II bound water is a product of strong hydrogen bonds between water molecules and resin network. The amount of Type II bound water, which is harder to remove and causes irreversible material changes, increases with higher temperature and longer exposure time. They also showed in [28] that Type I bound water softens the adhesive and lowers glass transition temperature (T_g). This behaviour has been observed by many other researchers as well (e.g. [25,29–32]). However, type II bound water was shown to lessen the extent of T_g depression in water saturated epoxy resins [28]. Correia [32] tested GFRP pultruded profiles with different resins in various environments and found two competing mechanisms responsible for T_g variation; plasticization mechanisms that tend to reduce T_g, and resin post-curing that was found to offset this effect.

2.2.2 Effect of moisture on fibre/matrix interface

Moisture can also wick along fibre/matrix interface, leading to formation of micro-cracks, and thereby loss of integrity [24,33–35]. Bradley and Garant [36] suggest that upon moisture sorption, the chemical bonding strength is initially reduced at the interface. Secondly, matrix subsequent swelling relaxes the existing residual stresses along the fibre/matrix interface, thereby deteriorating interfacial shear strength. The formed micro-cracks also act as new routes for moisture diffusion and accelerate damage growth [33]. Besides, the localized and separate micro-cracks were shown to coalesce and extend as a result of exposure to cyclic ambient environment [37].

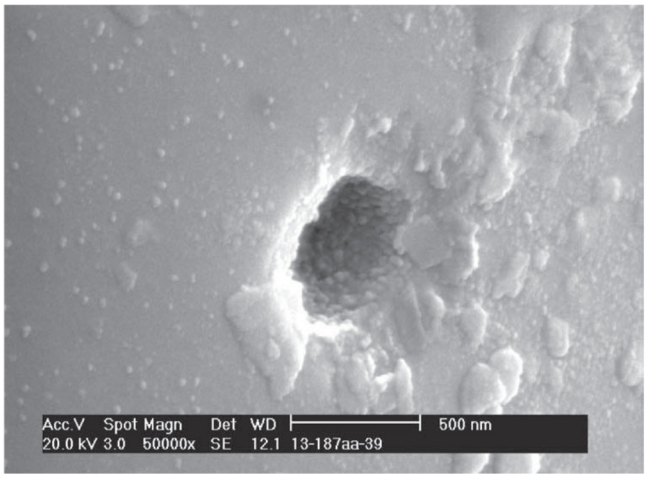

Figure 2.1. *Fibre pitting after immersion in water at 60 ˚C for 18 months* [38]

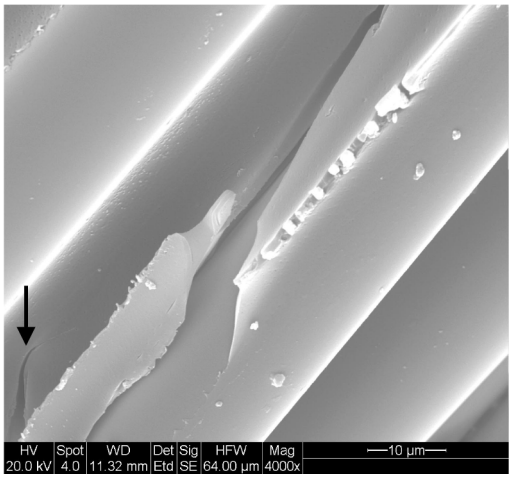

Figure 2.2. *E-Glass fibre level degradation* [39]

2.2.3 Effect of moisture on fibres

FRPs can also undergo degradation at the fibre level. In the case of glass fibres, moisture extracts ions from fibres, which can combine with water and serve as bases for etching and pitting of the altered fibre surface, see Figure 2.1 [38]. Upon longer exposures, damage growth of fibres continues through stress-corrosion mechanisms and cracking of the fibres, see Figure 2.2 [39]. Aramid fibres absorb moisture leading to accelerated fibrillation [16]. Carbon is chemically stable at normal temperatures and does not react with water or salts contained in sea water. However, similar to aramid and glass fibres, the carbon fibre/matrix interface can be degraded [40,41].

2.2.4 Effect of moisture on mechanical properties of FRP composites

The deterioration usually starts at the outer surface and depends on a number of factors such as manufacturing method, degree of cure, nature of surface finish and service environment [35,42]. Therefore, an additional surface coating is usually recommended to prevent micro-cracks at the surface. Extensive studies have investigated the effect of moisture on strength of FRP composite materials. While transverse properties, such as shear strength, is generally reported to undergo higher degradation levels, fibre-dominated properties, such as axial strength, are negligibly degraded in most cases [41]. Karbhari [24] predicts a negligible modulus change of the order of 10% over a period of 10-15 years for FRPs used in civil engineering applications. Immersion of high strength CFRP laminates in water at room temperature revealed an initial drop of 25-30% in tensile strength during first month of exposure, and remained constant during the rest of exposure period [43]. A decreasing trend for transverse tensile strength and increasing-decreasing behaviour for in-plane shear strength during the six-month exposure period was also observed, see Figure 2.3. It is also important to note that the degradation magnitude of mechanical properties becomes much larger when the interface or fibres are attacked. A study on the effect of moisture on bending strength of pultruded GFRP laminates showed 38% reduction for samples with damaged glass fibre/resin interface. The reduction was less than 20% for samples without apparent fibre/matrix failure [35].

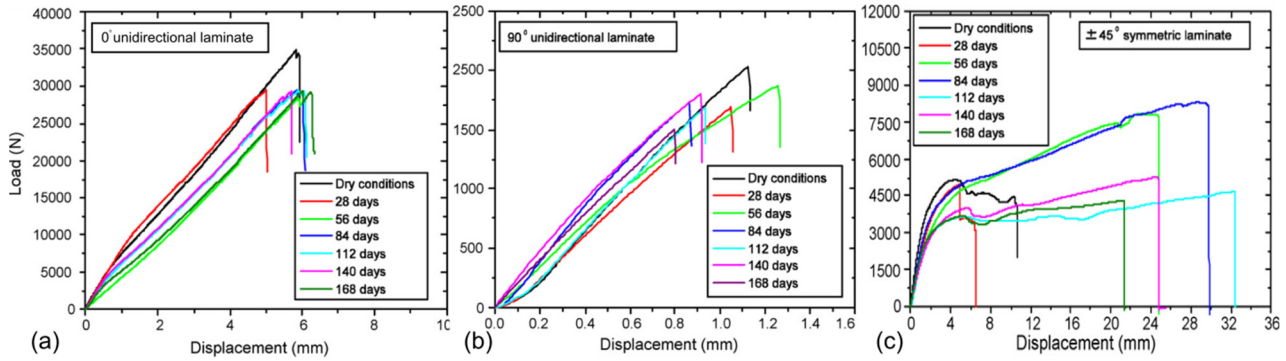

Figure 2.3. *Load vs. Displacement curves for dry and conditioned CFRP laminates; (a) 0°, (b) 90° and (c) ±45° unidirectional laminates, after* [43].

Experiments conducted by Scott and Lees [44] on dry and wet CFRP rods revealed that saturated CFRP tendons are likely to exhibit a reduced shear stiffness. However, the ultimate strength appeared to be fibre-dominated and was therefore less susceptible to reductions due to solution uptake effects. Gibbins and Hoffman [45] noted 20% reduction in shear strength after 121 days exposure of 2–3 mm thick laminates to 95% relative humidity at room temperature, whereas exposure of laminates to boiling water for 50 days resulted in a 40% reduction in the interlaminar shear strength (ILSS) [46]. Zhang and Mason [47] found that exposing 2.4 mm thick carbon fibre reinforced epoxy laminates to distilled water and synthetic sea water solution for 30 days at room temperature caused reductions of 6% and 10% in the ILSS, respectively. Akepati et al. [48] also found moisture playing a very significant role in the degradation of ILSS of carbon/epoxy composites. Similar behaviour has been also observed by others (e.g. [49–51]). However, Fourier transform infrared spectroscopy (FTIR) experiments have revealed that such degradations are to large extent due to physical phenomena such as plasticization of the polymeric matrix [32,52].

2.2.5 Moisture diffusion kinetics in FRP composites

Liao et al. [53] reviewed the durability of composites with particular attention paid to the materials of most interest for infrastructure applications. They concluded that the rate of degradation is in direct correlation with the rate of moisture sorption. Therefore, it is necessary for any long-term performance study to fully understand the mechanisms of moisture diffusion in these materials.

Moisture penetrates into composite materials by three different mechanisms [54,55]: (i) diffusion in polymer by transport of water molecules in holes of the polymer matrix via random molecular motion, (ii) capillary transport of water molecules along the fibre/matrix interface, (iii) moisture penetration into polymer matrix through micro-cracks and voids. The diffusion behaviour in amorphous polymers, which are commonly used in structural applications, was categorized into three classifications by Chin et al. [56]: (i) Fickian; (ii) swelling dependent; (iii) non-Fickian.

In many investigations, the Fickian diffusion is commonly adapted to predict moisture diffusion in composites. However, due to large variety of composite materials as well as larger diversity in exposure conditions, such as levels of relative humidity, temperature, and solutions, the literature thrives with data and analysis that report other sorption behaviours in polymeric composites. The most frequent deviations from the classical Fickian diffusion are illustrated in Figure 2.4 [57]. In this figure, curve LF corresponds to a Linear Fickian behaviour, while curves A and B represent a continuous gradual weight increase, and a two-stage diffusion due to relaxation effects [58], respectively. These moisture diffusion profiles generally lead to plasticization of composite, and are associated with reversible changes in material properties upon drying. Nevertheless, curves C and D represent irreversible degradation of the material due to damage growth such as fibre/matrix debonding, see Figure 2.5, and physical or chemical breakdown such as hydrolysis, respectively.

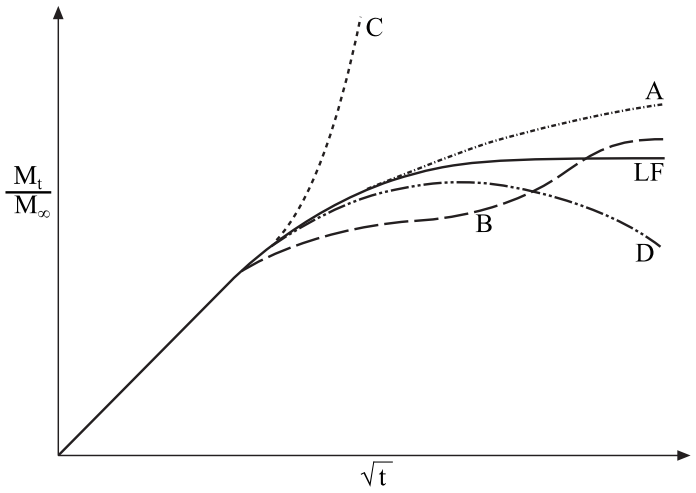

Figure 2.4. *The most frequent moisture uptake behaviours in polymers and composites, after* [57] *(Slightly modified)*

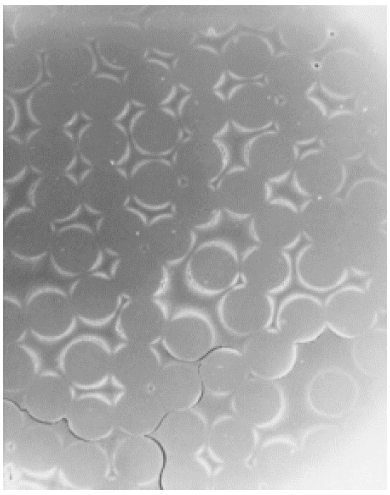

Figure 2.5. *Moisture-induced debonding at the fibre/matrix interface, after* [57]

Although investigations on moisture diffusion in fibre-reinforced composites used in civil engineering applications are very limited, the available data suggests Fickian behaviour (curves LF, A and B) up to saturation. However, after reaching saturation, a non-Fickian behaviour with weight-loss or regain (curves D and C) is usually observed, irrespective of resin type [24,40,59,60]. A Langmuir-type model has also been shown to fit the dual-stage diffusion data from a series of glass/vinyl-ester laminate systems immersed in deionized water at various temperatures [38]. Moreover, the results of an inverse analysis approach showed that while the diffusivity is highly dependent on temperature, the maximum moisture content mainly depends on relative humidity [61].

Prolonged exposure of FRP composites to humidity at high temperatures has shown to cause material weight loss. The weight loss in polyester systems is mainly due to hydrolysis and resin dissolution [25], whereas the mass loss of vinyl-ester systems is attributed to the leaching of low-molecular-weight elements [39,62]. In addition, Weitsman [33] presented cyclic exposure data for various composites exposed to ambient fluid environments. He noted an increasing divergence of the classical predictions from the experimental data with increasing number of cycles. It was postulated that the observed disparity stems from moisture-induced damage at fibre/matrix interface and was explained by a combined damage/diffusion model. The diffusion kinetics in FRP composites also depends on the orientation of fibres. Raha and Ranganathaiah [63] studied the diffusion kinetics in epoxy/glass (0°) and (45°) fibre oriented composites that resulted in change of diffusion mode from curve LF to curve B, respectively. Pierron et al. [64] also noticed an extremely larger diffusion rate along the fibre direction than that in transverse to the fibre direction, which was attributed to the preferential path-way for moisture provided by fibre/matrix interface. The existence of voids can also significantly increase the mass uptake in FRP composites. Thomason [65] showed that the presence of only 1% voids, can double moisture

uptake as compared to a void-free GFRP composite. As a result, larger strength reductions with increasing voids has been witnessed in several studies [29,66].

FRP structures in civil engineering applications can also be exposed to de-icing salt solutions or salt water. Robert et al. [67] immersed glass fibre reinforced polypropylene thermoplastic composite laminates (PP/Glass) in tap water and salt solution at various temperatures. It was observed that for a given immersion time, the salt solution absorption was generally lower than that of tap water. However, immersion in a salt solution had a greater effect on flexural properties than immersion in tap water. Microscopic pictures indicated that the NaCl solution significantly affects the composite by degrading the fibre/matrix interface [30]. Lower moisture uptake and slightly larger degradation in sea water solutions than in distilled water was also found by other researchers for various polyester, vinyl ester and epoxy composites [30,36,40,68,69]. Nevertheless, Davies et al. [69] noted that while permanent damage was induced in the polyester composites after 18 months of water immersion, the epoxy and vinyl-ester shear properties were much less affected by ageing and were largely recovered after drying. The larger degradation of polyester composites in seawater is attributed to hydrolysis of polymer matrix and fibre/matrix interface, and can be alleviated by using vinyl-ester or epoxy-based composites [70].

Nanoparticles have been recently used to improve durability of FRP composites by lowering polymer permeability and thus moisture ingress [71–75]. Although the effectiveness of these materials is approved, their utilization in construction industry is expensive and is only limited to very special cases [4].

The moisture uptake characteristics of various epoxy-based FRP composites fabricated by wet-layup process and adhesive bonding through prefabrication are presented in Table 2.1. As can be seen, in the case of prefabricated systems, the maximum moisture uptake (M_{max}) is significantly lower than the obtained levels in the wet-layup based systems. This is mainly

Table 2.1. *Moisture uptake characteristics of various epoxy-based unidirectional FRP composite systems for civil engineering applications*

Composite system	Process	Fibre volume[%]	Distilled water 23 °C		Salt water 23 °C		Distilled water 38 °C	
			M_{max}[%]	D_c[mm^2/s]	M_{max}[%]	D_c[mm^2/s]	M_{max}[%]	D_c[mm^2/s]
E-Glass/epoxy1	WL[1]	28	3.07	4.26E-8	2.86	3.09E-8	3.77	7.25E-8
Carbon1/epoxy1	WL	33	2.80	2.62E-8	2.66	2.29E-8	3.62	5.20E-8
Carbon2/epoxy2	WL	27	1.40	3.00E-8	1.06	4.45E-8	1.38	1.46E-7
Carbon2/epoxy3	WL	32	2.42	4.13E-8	1.83	3.09E-8	2.06	2.91E-7
Carbon3/epoxy4	WL	29	2.01	3.77E-8	1.73	3.57E-8	2.14	8.03E-8
Carbon4/epoxy5	WL	26	2.51	2.08E-8	2.37	3.05E-8	2.81	6.93E-8
Carbon4/epoxy5	WL	34	3.08	2.45E-8	3.29	2.95E-8	3.32	7.02E-8
Prefabricated CFRP1	AB[2]	62	0.52	8.77E-9	0.36	7.15E-9	0.55	2.26E-8
Prefabricated CFRP2	AB	61	0.30	5.18E-9	0.31	5.74E-9	0.34	3.69E-8
Prefabricated CFRP3	AB	69	1.09	7.67E-9	0.55	5.38E-9	1.56	3.49E-8

[1]Wet Layup

[2]Adhesive Bonding through prefabrication

due to the higher fibre volume fractions as well as the use of elevated cure regimes during fabrication. It is also apparent that the system with glass fibres exhibit higher diffusivity (D_c) and maximum moisture content as compared to the similar system with carbon fibres. Further details as well as mechanical degradation levels of the investigated composite systems can be found in [76].

2.3 Effect of moisture on epoxy adhesive

Due to the ability of epoxy adhesives to cure at room temperature, they are commonly preferred to other resins in civil engineering applications [77]. In addition, curing of epoxy adhesives is accompanied by low shrinkage which is advantageous for the case of metallic substrates [78]. However, standard epoxy formulations are highly susceptible to moisture absorption and can absorb moisture between 1 to 7 percent of their weight [79].

2.3.1 Effect of moisture on mechanical properties of epoxies

The diffused water through adhesive is the primary route of moisture ingression in adhesively bonded joints. Having gained access, water can weaken adhesive by one or a combination of the following mechanisms:

- Altering adhesive in a reversible manner, e.g. plasticization;
- Irreversibly altering adhesive, e.g. hydrolysis, cracking or crazing
- Additional stresses induced by swelling of adhesive.

The high moisture absorption susceptibility of epoxy adhesives stems from epoxy surface topology [80] and resin polarity [81]. Soles et al. [80] found that moisture initially penetrates into the epoxy structure through the inherent nanovoids of the epoxy surface topology, which vary from 5.0 to 6.1 Å in diameter. Water molecules have an average diameter of 3.0 Å and can easily enter epoxies. The resin polarity of epoxies is due to the presence of hydrophilic groups that attract highly polar water molecules through hydrogen bonding. The adsorbed moisture interrupts the molecular chain of polymers and results in degradation of mechanical properties based on moisture concentration. On the one hand, the moisture induced plasticization causes depression of glass transition temperature (e.g. [82,83]). This is primarily important for cold cured adhesives that have generally glass transition temperatures less than 60 °C in the dried stage [84]. Hence, further depression of T_g makes it closer to normal service temperatures in some environments, and endangers the joint overall stability. On the other hand, the expansion forces exerted by moisture while stretching polymeric chains creates differential strains that result in swelling [85,86]. For the case of adhesively bonded joints where the adhesive is sandwiched between two substrates, swelling will lead to internal residual stresses [87]. A linear relation between swelling and moisture content has been observed by many researchers for various adhesive systems [88].

The modulus and strength of polymer adhesives is also known to deteriorate as a consequence of moisture-induced plasticization [77,89–96]. Typical stress-strain curves for dog-

bone adhesive samples, before and after exposure to humid environments, are schematically depicted in Figure 2.6. Knox and Cowling [21] found that under laboratory ageing conditions (30 °C, 100% relative humidity), the strength and modulus of bulk adhesive samples degraded by 20% and 10%, respectively. Nguyen et al. [89] found more significant degradation of a different epoxy adhesive as a result of exposure to 20 °C and 50 °C seawater, where the stiffness reduced to 65% and 45% of the initial value, respectively. Lapique and Redford [97] also noted increased maximum strain and ductility of aged adhesives. Bordes et al. [98] plotted the adhesive modulus as a function of moisture content and found a direct correlation between them without any clear influence from ageing environment or solution, see Figure 2.7. Moreover, Lin and Chen [99] conducted a series of cyclic hygrothermal ageing tests on an epoxy adhesive, and observed that the elastic modulus reduction of the saturated, desorbed, and re-saturated group samples are 29.45, 8.92 and 41.5%, respectively, compared to the unaged group samples. This observation could be attributed to the increased plasticization effect with hygrothermal history. Roy et al. [100] investigated the reversibility of these effects and observed that drying epoxy adhesive samples aged at 40 °C in water not only restores the 20% drop in tensile modulus, but also would cease the plasticity. They suggest that water extracts additives that plasticize the epoxy resin and this property of adhesive is lost after cyclic moisture exposure.

Due to the increased ductility and enhanced crack-tip blunting mechanisms, the fracture toughness of adhesives generally increases with absorbed water [77,101]. However, many studies have shown that cohesive strength of adhesives drops with increasing moisture content (e.g. [23,102,103]), see Figure 2.8. Johnson and Butkus [103] found a reduction of 70 percent in mode I fracture toughness of an epoxy adhesive upon exposure to hot/wet conditions. In another study, Loh et al. [104] noted steady reduction of mechanical and fracture properties of an epoxy adhesive with increasing moisture content. As the samples were aged at different humidity levels and exposure times, it was also concluded that these properties depend solely on moisture content. In the case of cyclic hygrothermal exposure tests, fractographic analysis revealed that the absorbed moisture can change the fracture mechanisms

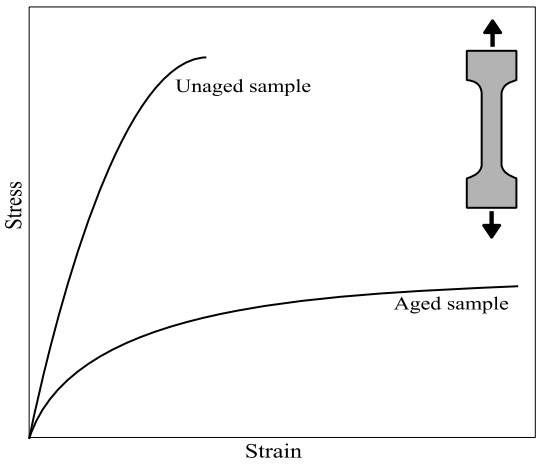

Figure 2.6. *Typical effect of moisture on tensile response of adhesives*

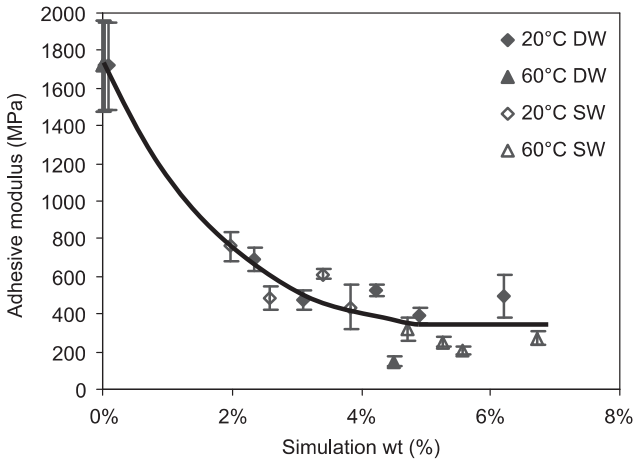

Figure 2.7. *Modulus attenuation versus water content; DW (deionized water) and SW (salt water), after* [98]

of the polymer from brittle to ductile for the unaged and saturated specimens [99]. The authors reported a re-transform of fracture mechanisms from ductile to brittle after drying of saturated specimens.

2.3.2 Moisture diffusion kinetics in epoxy adhesives

The diffusion process in adhesives is similar to that for polymer matrices in FRPs. The moisture uptake depends on solution concentration, time, sheet thickness, and temperature. It has been shown for various adhesives that the rate of diffusion follows Fick's first law [105], see Figure 2.9. However, anomalous diffusion behaviour after the initial moisture uptake has been reported for some adhesives at temperatures below T_g [60,98,106,107]. Several models have been proposed to predict such behaviour, including dual Fickian (relaxation-dependent) [108,109], delayed dual Fickian [110], concentration-dependent [111], time-dependent [112], and Langmuir model [58,113]. Glaskova et al. [112] investigated the accuracy of a number of these models for a selected epoxy and found the Langmuir and dual Fickian models to be particularly accurate. Furthermore, Mubashar et al. [114] studied the cyclic moisture behaviour in an epoxy adhesive and observed that while the sorption process was non-Fickian, the desorption was Fickian. Other studies have also shown faster desorption and re-sorption processes in the case of cyclic moisture exposure [99,110,114]. Therefore, for a more accurate moisture profile prediction in adhesive joints, it is essential to consider history-dependent parameters of moisture-uptake data. It is noteworthy that despite different observations regarding moisture uptake profiles in adhesive samples, it is well accepted that higher temperatures accelerate diffusion, while saturation moisture content depends on humidity content and solution type.

Immersion of epoxies in salt water solutions generally results in lower saturation moisture content than distilled water [56]. However, some researchers have found an opposite trend [115] or similar diffusivity for both cases [113]. As the literature is inconclusive, the presence of salt in an aqueous exposure environment could either increase or decrease the rate of

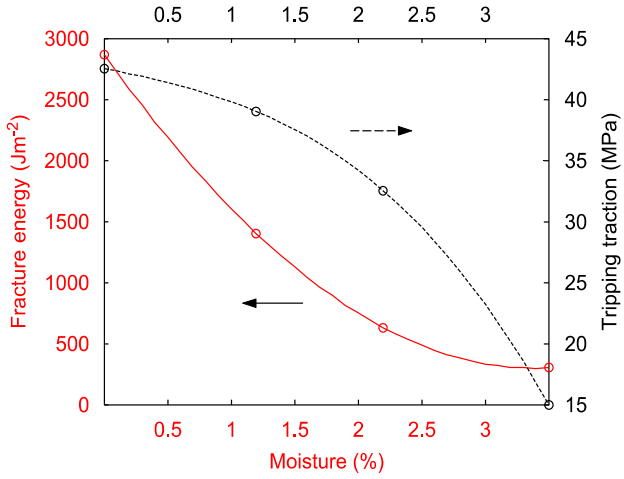

Figure 2.8. *Moisture dependent tripping traction and fracture energy, after* [102]

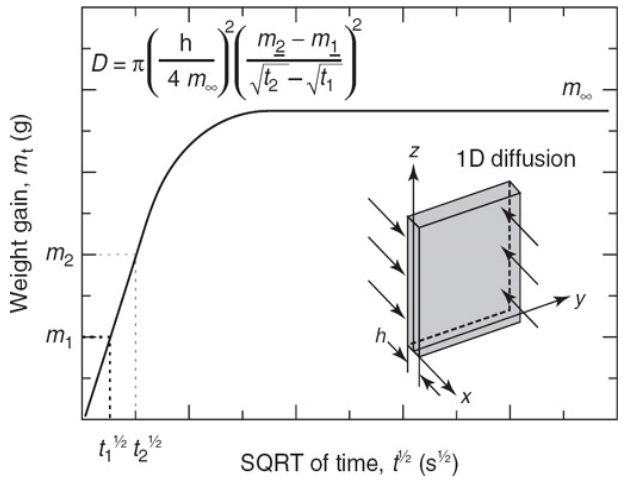

Figure 2.9. *Theoretical absorption curve and one-dimensional Fickian diffusion parameters* [105]

uptake and equilibrium moisture content, depending on solution concentration, chemistry of epoxy, cure state, and exposure temperature.

The moisture uptake data for a number of common structural adhesives used in civil engineering applications are collected in Table 2.2. Such data are usually obtained by gravimetric tests which are based on periodic measurements of the weight of immersed adhesive films.

Table 2.2. *Moisture uptake data for a number of common structural adhesives in civil engineering applications*

Adhesive	Exposure environment	Diffusion behaviour	Initial D_c [mm^2/s]	M_{max} [%]
Sikadur 30: Two-part epoxy adhesive [76]	23 °C Deionized water	Dual Fickian	3.41×10^{-8}	0.98
	23 °C Sea water	Dual Fickian	6.15×10^{-8}	0.29
	37.8 °C Deionized water	Dual Fickian	1.12×10^{-7}	2.17
	60 °C Deionized water	Sigmoidal	4.59×10^{-7}	6.83
SCCI: Epoxy adhesive [76]	23 °C Deionized water	Dual Fickian	4.19×10^{-8}	3.00
	23 °C Sea water	Dual Fickian	4.59×10^{-8}	3.00
	37.8 °C Deionized water	Dual Fickian	1.82×10^{-7}	2.70
	60 °C Deionized water	Sigmoidal	8.97×10^{-7}	2.20
FYFE: Solids filled epoxy adhesive [76]	23 °C Deionized water	Dual Fickian	4.80×10^{-7}	2.91
	23 °C Sea water	Dual Fickian	2.32×10^{-7}	2.24
	37.8 °C Deionized water	Dual Fickian	1.48×10^{-6}	5.34
	60 °C Deionized water	Sigmoidal	1.19×10^{-5}	26.4
FYFE: Two-part epoxy adhesive [76]	23 °C Deionized water	Dual Fickian	6.69×10^{-8}	2.44
	23 °C Sea water	Dual Fickian	5.63×10^{-8}	2.20
	37.8 °C Deionized water	Dual Fickian	1.84×10^{-7}	2.52
	60 °C Deionized water	Sigmoidal	9.92×10^{-7}	2.19
Araldite 420: Two-part epoxy adhesive [89]	20 °C Sea water	Linear Fickian	3.43×10^{-8}	3.86
	50 °C Sea water	Linear Fickian	2.07×10^{-7}	5.94
Araldite 2015: Two-part epoxy adhesive [98]	20 °C Deionized water	Linear Fickian	4.69×10^{-8}	7.00
	20 °C Sea water	Dual Fickian	8.02×10^{-8}	4.45
	40 °C Deionized water	Linear Fickian	2.20×10^{-7}	8.00
	60 °C Deionized water	Dual Fickian	1.15×10^{-6}	8.43
	60 °C Sea water	Dual Fickian	1.38×10^{-6}	4.60

2.4 Effects of moisture on adhesively bonded joints

In addition to the durability aspects of FRP and adhesive, the stability of the interface between adhesive and substrate is a crucial factor regarding the long-term performance of bonded FRP/steel joints [19]. On the one hand, the interfacial moisture diffusion is known to occur at much faster rates compared with the diffusion through the adhesive [116,92,117–122]. On the other hand, the interfacial adhesion between steel substrates and adhesives are categorized as unstable in the presence of moisture [123]. Additional factors that may accelerate degradation of the interface are cathodic corrosion, galvanic corrosion and poor surface treatment. Unfortunately, all of the abovementioned factors are very complex phenomena that are not fully understood to date [124].

Due to the moisture permeability of FRP composites, a shorter moisture diffusion path is provided through the surface of adherends to the interface. This phenomenon is not broadly investigated as the majority of the available research are mainly conducted within fields such as aerospace and automobile industry where aluminium is the most commonly used adherend. Recently, a comparison between the moisture content of adhesive joints with permeable and impermeable adherends has been performed by Hua et al. [125] where a significant increase in the moisture content is found for the former case.

Another common observation is a shift of failure locus to at or near the adhesive/steel interface, or to the FRP adherend. The mechanisms that lead to such behaviours are adhesive/steel bond disruption and interlaminar shear strength degradation of FRP composites, respectively. These mechanisms along with the most recent long-term performance tests on adhesively bonded FRP/steel joints used in civil engineering applications are thoroughly discussed in Paper I.

Despite the commonly reported deleterious effects of moisture on strength of bonded joints, there has been evidence that small amounts of moisture can be beneficial in joints with stable adhesive/steel bonds [126–128]. The reason is that the plasticized adhesive distributes stresses over a larger area in the joint that would in turn decrease the peak stresses. This behaviour is investigated in Paper III.

3 Overview of experimental programme

Figure 3.1 shows the flowchart of the experimental programme presented in this thesis. To address the aims of the study, the experimental programme is divided into two main branches:

(1) experiments aimed at characterizing the environmental effects at material-level,
(2) long-term performance experiments aimed at studying the behaviour of environmentally aged joints.

The material characterization tests are designed to obtain moisture diffusion as well as environmentally dependent mechanical properties of the materials used to fabricate bonded FRP/steel joints. Standard gravimetric measurements were modified and used to obtain 1D and 3D diffusion characteristics. Tensile and fracture properties were also obtained by testing material coupons and fracture-mechanics bonded configurations, respectively. The outcome of these tests serves as the input data for the numerical analysis. The long-term performance experiments include adhesively bonded CFRP/steel and GFRP/steel double lap shear joints. In addition to providing valuable information about the degradation mechanism in a joint-level, these tests will be used to verify the numerical analysis.

In order to find the contribution of different environmental factors and possible synergies, the following exposure scenarios were planned: (i) water immersion vs. high relative humidity levels, (ii) exposure to de-icing salt solutions likely to occur in bridges, (iii) temperature as an accelerating factor as opposed to ambient temperature conditions, (iv) cyclic wet/dry exposure scenarios, (v) freeze/thaw cycles in the presence of moisture, (vi) freeze/thaw cycles in dry conditions. The experiments under the exposure conditions (i) to (iv) are ongoing, whereas the freeze/thaw exposures will be performed in the continuation of the project.

3.1 Materials

Four materials were utilized in this study: epoxy adhesive, GFRP laminate, CFRP laminate and normal strength carbon steel (S355). The used adhesive is a commercial two part structural epoxy adhesive, STO® BPE Lim 567 that is used in structural applications. This epoxy is one of the few commercially available structural adhesives that is described compatible with steel. The GFRP material was manufactured by pultrusion process and cut from the ASSET FRP bridge deck elements produced by Fiberline Composites®. The GFRP laminates were supplied as rectangular plates with the nominal dimensions equivalent to 50×400×10 [mm] (width × length × thickness). Pultruded unidirectional normal-strength CFRP laminates were manufactured by Mostostal® with a nominal thickness of 1.25 mm and width of 50 mm.

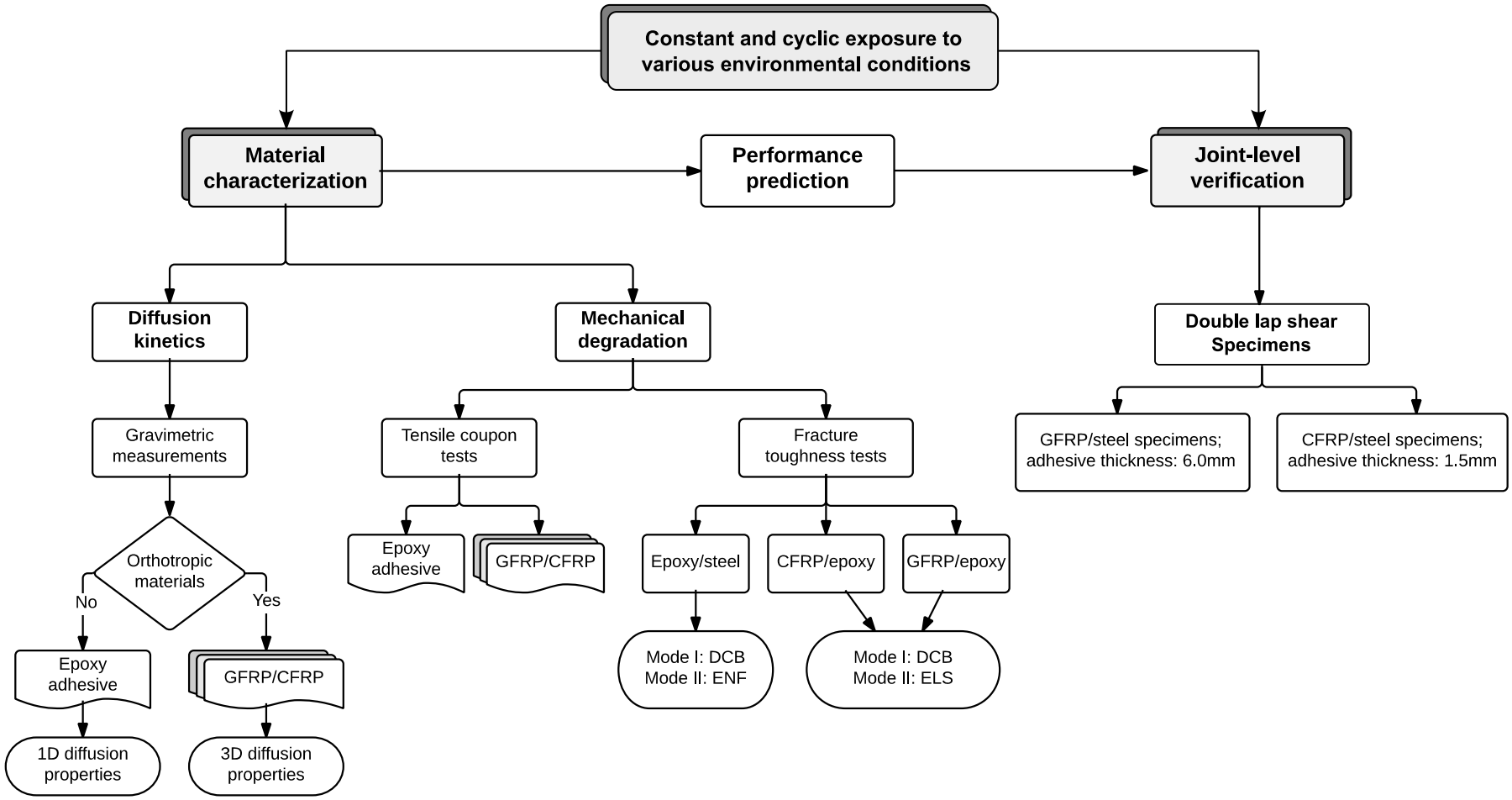

Figure 3.1. Flow chart of the experimental programme

4 Material characterization tests

4.1 Dynamic mechanical analysis (DMA)

The glass transition temperature of adhesive is an important parameter that has to be taken into account prior to designing environmental exposure scenarios. It is recommended in [129] and [130] to limit the maximum exposure temperature to 5-15 °C below T_g.

DMA is a powerful tool to investigate the temperature effects on material stiffness. For viscoelastic materials, such as polymers, the temperature at which material stiffness drops significantly (T_g) is of interest and can be obtained by means of DMA analysis. The common procedure involves dynamic loading of specimen within the material elastic region while the temperature is increased. During the dynamic loading, a sinusoidal stress is applied to the material and a resultant sinusoidal strain as well as a phase difference (δ) are measured. For viscoelastic materials, the modulus can be divided into an elastic component, storage modulus (E'), and a viscous component, loss modulus (E''). Storage modulus is related to specimen's stiffness and is the pertinent parameter to be studied when change of material's elastic stiffness with increasing temperature is of interest. The tangent of phase difference, $tan(\delta)$, is another common parameter that is commonly used to get the relationship between the elastic and inelastic components.

In this study, the T_g of the used epoxy adhesive was measured using DMA analysis. To prepare the specimens, adhesive was mixed and casted into a square moulding form with a thickness of 1 mm. After it was fully cured, three specimens with the average dimensions of 13.5 × 6.3 (mm) were cut from the plate. The DMA tests were carried out on three epoxy adhesive specimens using a TA Instruments® DMA Q800 machine, see Figure 4.1. The oscillatory strain amplitude of 0.01 % was applied at a frequency of 1 Hz on a tensile setup while the sample were heated up at a rate of 2 °C/min from 25 °C to 100 °C. The

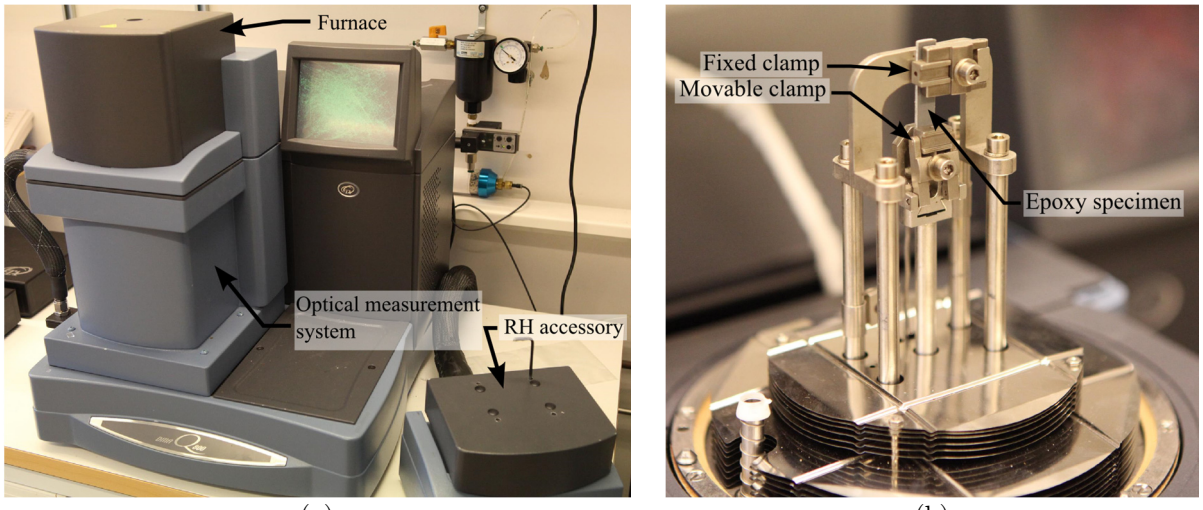

(a) (b)

Figure 4.1. *DMA tests: (a) Q800 machine; (b) specimen setup inside furnace.*

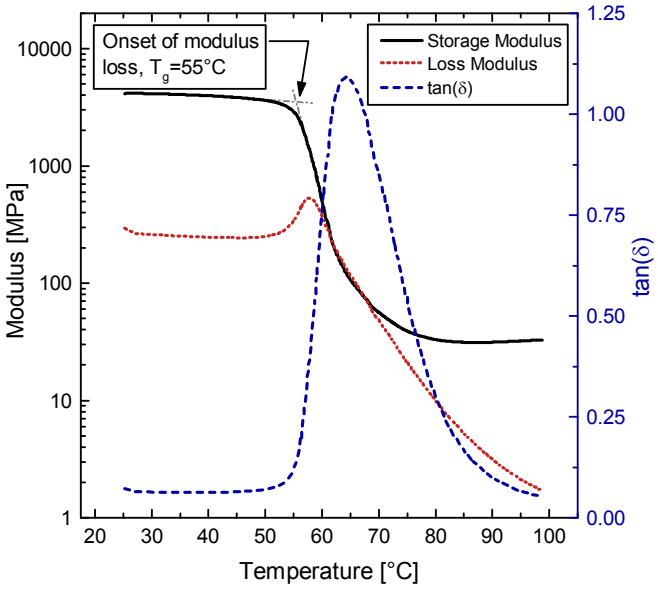

Figure 4.2. *DMA test results for STO BPE lim 567 adhesive.*

average results for all specimens are plotted in Figure 4.2. It can be seen that the onset of storage modulus loss is at 55 °C, while the peak of *tan(δ)* is found at 65 °C. Although both of these values can be interpreted as T_g of adhesive, the former is more meaningful in a mechanical sense. Thus, $T_g = 55$ °C was considered for the adhesive, and the exposure scenarios were designed accordingly.

4.2 Moisture diffusion characterization

4.2.1 Exposure scenarios and specimens

Table 4.1 lists the exposure scenarios that were utilized to obtain the moisture diffusion characteristics of the used adhesive and FRP composites. In addition, the following aspects were also investigated: (i) the effect of increasing temperature, as an accelerating factor, on diffusion kinetics; (ii) the effect of salt water solutions that are expected in bridge environments; (iii) the comparison of immersion versus high relative humidity levels on diffusion behaviour; (iv) the effect of cyclic exposure conditions.

Table 4.1. *Exposure scenarios utilized in the diffusion characterization tests.*

Temperature	Humidity level	Solution	ID
45 °C	Immersion	5% NaCl	45 SW
45 °C	Cyclic Immersion/Drying	5% NaCl	45 SW-CY
45 °C	Immersion	Distilled Water	45 DW
45 °C	Cyclic Immersion/Drying	Distilled Water	45 DW-CY
45 °C	95% Relative Humidity	Distilled Water	45 RH
45 °C	Cyclic 95% RH/Drying	Distilled Water	45 RH-CY
20 °C	Immersion	5% NaCl	20 SW
20 °C	Immersion	Distilled water	20 DW

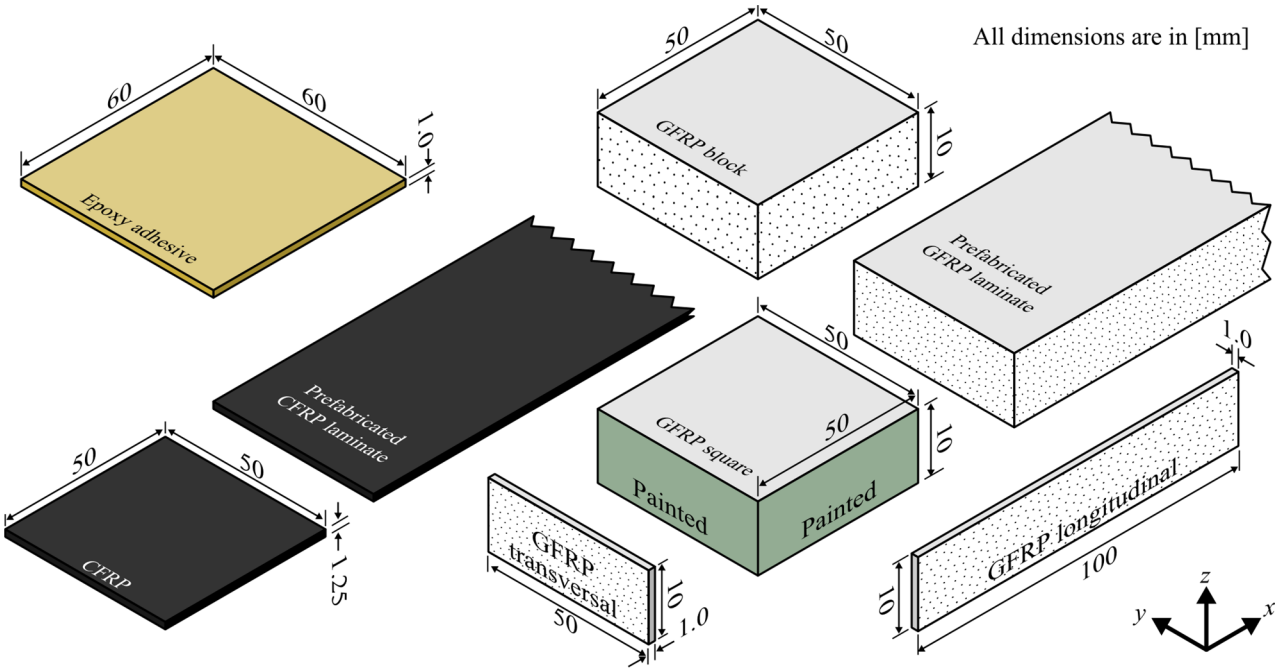

Figure 4.3. *Schematics of specimens used in the gravimetric measurements*

Schematics of the specimens used for gravimetric measurements are illustrated in Figure 4.3. Three replicas were included for each ageing condition. As can be seen, the GFRP and CFRP specimens were cut from prefabricated laminates provided by the manufacturers. Water jet cutting technique was used to cut the specimens into pieces to minimize the plausible mechanical and thermal damages caused by other cutting methods. As the GFRP material is orthotropic, additional specimens were included to characterize the moisture diffusion in all three dimensions. A GFRP block configuration was also included to verify 3D mass diffusion analysis discussed in Section 8. The thickness of the provided CFRP laminate is considerably smaller than its other dimensions, and thus, one-dimensional diffusion can be considered.

The adhesive specimens were manufactured by casting epoxy into Teflon moulds and curing them for one week in the room environment. Moreover, an additional series were included to investigate the effects of fast curing on moisture diffusion behaviour of adhesive. These series were cured in an oven at 60 °C for 48 hours and are identified with “FC” suffix. More information about the specimen manufacturing and measurement procedures can be found in Paper III.

4.2.2 Moisture diffusion into epoxy adhesive material

Once the specified curing time was reached, the epoxy adhesive specimens were first weighted and then directly exposed to the aforementioned exposure scenarios. It should be mentioned that the specimens that had been left in the room environments to cure were not dried prior to exposure to reproduce in-service conditions. The gravimetric measurements were performed periodically for up to a year according to ASTM D5229/D5229M-14

[131]. In case of cyclic exposure scenarios, the specimens were removed from the exposure conditions upon reaching saturation and stored in an oven at 45 °C to dry. The saturation level is defined as when the average moisture content of the material changes by less than 0.020 % over two consecutive reference time period spans. During the drying cycle, the periodic weight measurements were continued.

The moisture uptake data for epoxy adhesive specimens after one year of exposure to constant conditions are plotted in Figure 4.4. The best Fickian fit of the experimental data are plotted with lines for which the derived coefficients will be used in the mass diffusion simulations (Section 8 and Paper III). As can be seen, the moisture diffusion rate (initial linear slope of the curves) is a function of temperature of exposure conditions and is independent of the solution type or concentration. However, the same ageing solutions have led to similar final moisture saturation levels. Moreover, the lowest and highest moisture saturation contents are obtained for vapour (45 RH) and distilled water conditions, respectively. Comparatively, the absorption in salt water solution is found less than distilled water. Furthermore, while fast curing of the adhesive has led to slightly higher moisture saturation contents at 45 °C exposure conditions, it has reduced considerably at 20 °C DW. These observations are thoroughly discussed in Paper III.

The moisture absorption and desorption curves of cyclic exposure scenarios are plotted in Figures 4.5 to 4.7. As can be seen, after several cycles of absorption at 45 °C 95%RH and desorption in the oven, the moisture diffusion into adhesive still follows the Fickian behaviour. However, notably after the first drying cycle, the moisture content of specimens cured at room temperature has become less than zero. Consequently, these specimens obtain a higher moisture content at saturation at the end of the second wetting cycle. On the contrary, the fast cured specimens exhibit repeatable behaviour during all the cycles, see Figure 4.6(a) and Figure 4.7(a). This behaviour is explained by the fact that the specimens cured

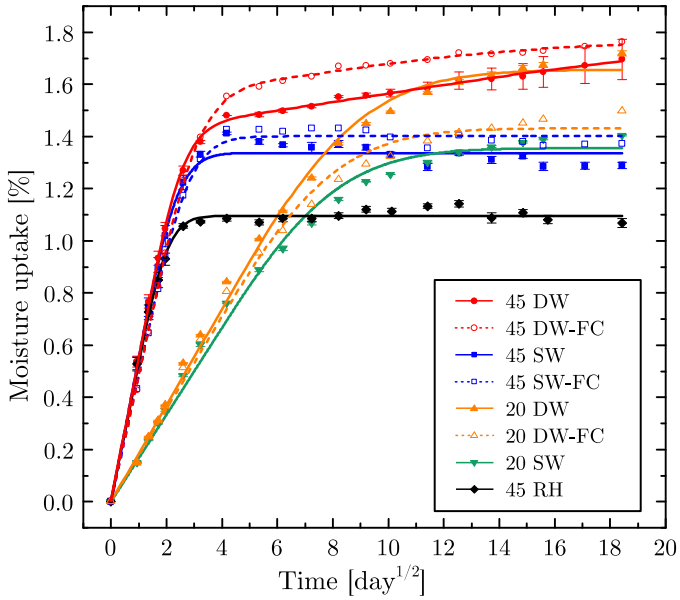

Figure 4.4. *Moisture uptake data for the epoxy adhesive specimens*

at the room temperature were not dried prior to exposure. Hence, they might have contained initial moisture content that was not removed until the end to the drying cycle. The fast cured specimens were kept in an oven at 45 °C, and, thus, have had precisely zero present moisture content at the beginning of the tests. Therefore, it can be concluded that as long as the adhesive is fully cured, the curing method does not influence the cyclic diffusion behaviour. Nevertheless, fast curing at higher temperatures than room environment can remove the initial moisture content of adhesive.

The Fickian diffusion model was fitted to the experimental data. It can be seen that this model provides an excellent fit to absorption, desorption and resorption plots, see Figures 4.5 to 4.7. The changes of the obtained Fickian moisture diffusion coefficients during

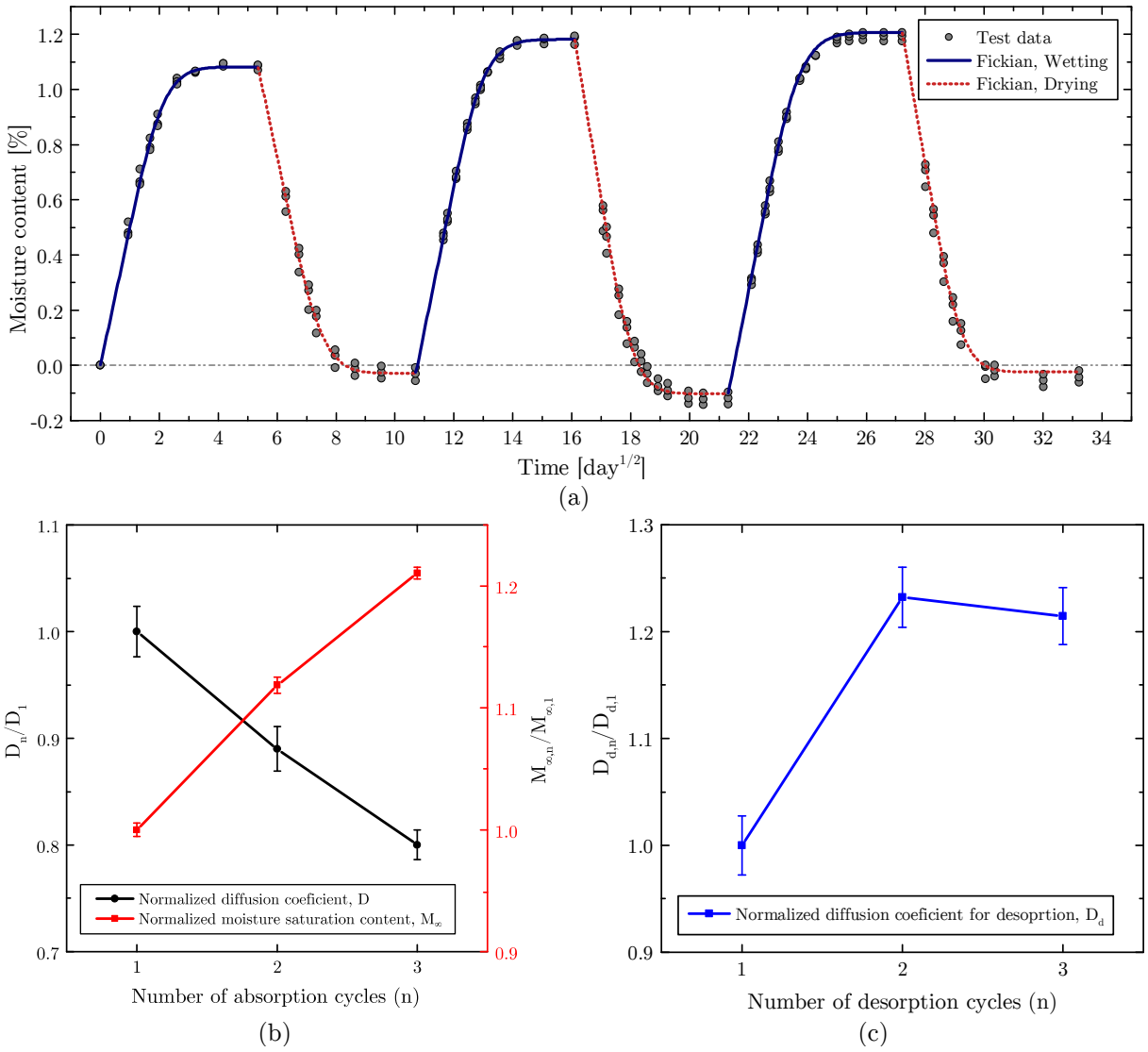

Figure 4.5. *Epoxy adhesive exposed to cyclic conditions; wetting at 45 °C 95% RH and drying in oven at 45 °C: (a) moisture absorption and desorption curves; (b) changes of obtained moisture diffusion characteristics during absorption cycles; (c) changes of obtained diffusion coefficients during desorption cycles.*

absorption and desorption cycles at 45 °C 95% RH are plotted in Figure 4.5(a) and (b), respectively. During the absorption cycles, the moisture saturation content raises with increasing number of cycles which consequently hinders the diffusion process and lowers the diffusion coefficient. The increased saturation content can be attributed to the removal of the initial moisture content during the initial stages. In addition, with increased exposure cycles, the polymer chains may have got damaged, leading to an increase of available sites for absorption. The initial moisture content is removed after the first drying cycle, which leads to an almost constant diffusion coefficient during the next desorption cycles.

The absolute value of moisture content during the cyclic immersion exposure conditions are shown in Figure 4.6(b) and Figure 4.7(b). It is apparent that in both distilled water and salt water solutions, the absorption is slower than the desorption rate which is consistent with earlier studies (e.g. [114]). Moreover, it can be seen that the diffusion rate during the wetting cycles has remained constant.

In conclusion, the results presented in this section suggest that for accurate simulation of the moisture profile in adhesive joints, it is essential to obtain history-dependent diffusion properties. However, for the adhesive investigated in this study, if the initial moisture content is removed before exposure, such dependency becomes less prominent and can be neglected.

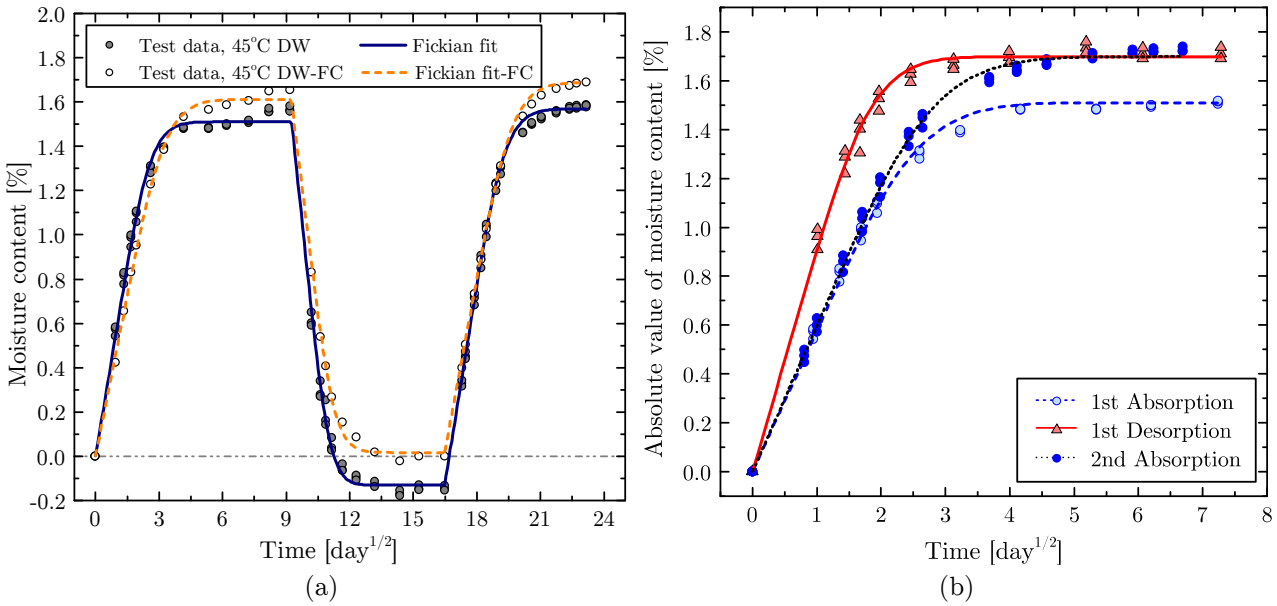

Figure 4.6. *Moisture absorption and desorption curves for epoxy adhesive conditioned in distilled water at 45 °C: (a) sequential mass uptake data; (b) absolute value of moisture content for each exposure cycle of adhesives cured at room temperature.*

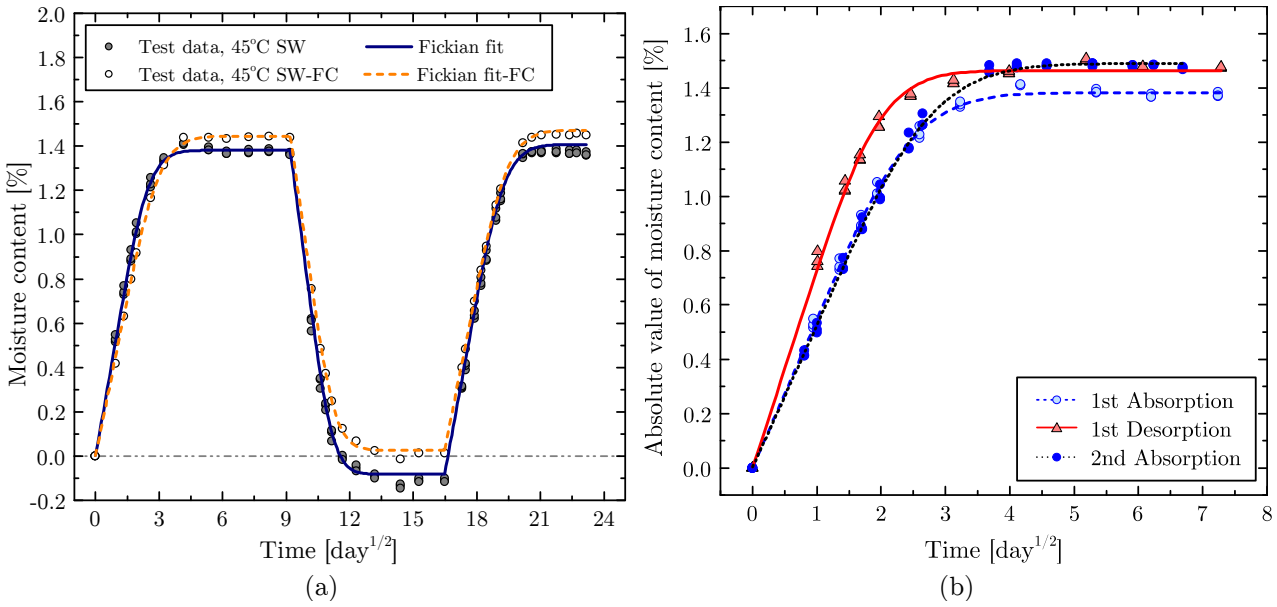

Figure 4.7. *Moisture absorption and desorption curves for epoxy adhesive conditioned in salt water at 45 °C: (a) sequential mass uptake data; (b) absolute value of moisture content for each exposure cycle of adhesives cured at room temperature.*

4.2.3 Moisture diffusion into FRP composites

Figure 4.8 depicts the typical stack layup and cross-section view of the pultruded GFRP composites used in this study. A polyester surface veil covers the outside and protects the inner layers against environmental attacks. According to the manufacturer's description, the cross section consists of approximately 62% E-glass fibres embedded in an isophthalic polyester resin. Due to such orthotropic structure, it may be expected that the material

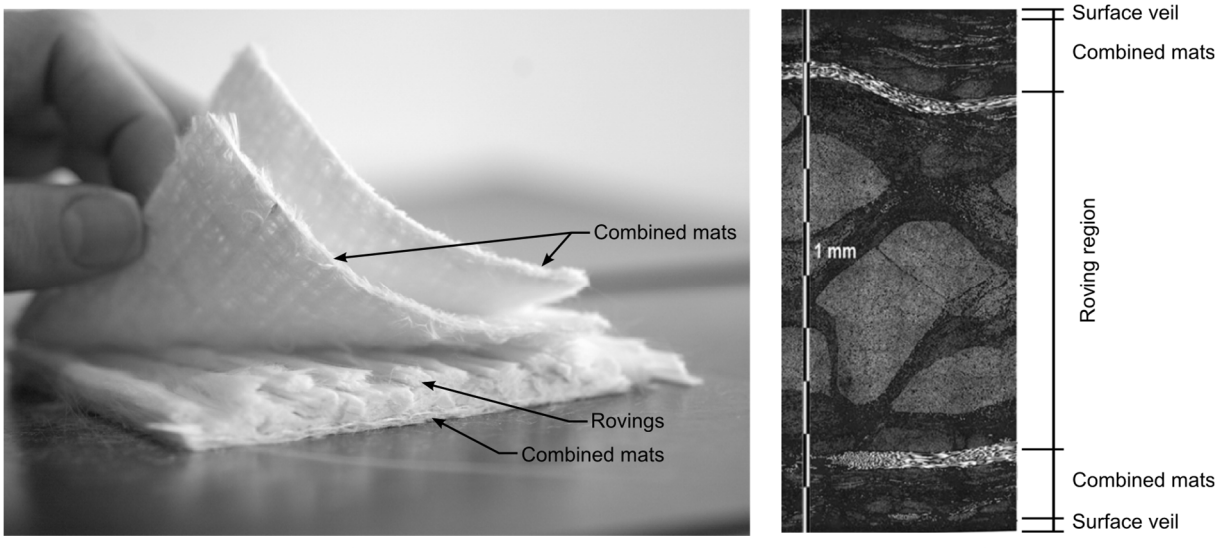

Figure 4.8. *Typical fibre architecture and cross-section view of pultruded GFRP composite (CCLab, EPFL); slightly modified.*

exhibit different diffusion behaviour in each spatial direction. The CFRP laminates consist only of unidirectional carbon fibres embedded in VORAFORCE^{TM} TP 201 epoxy resin. As a result, these laminates are considerably thinner than the GFRP specimens.

The moisture diffusion results of all the FRP composites are reported completely in Paper III. Herein, a summary of the results and a short discussion is presented. All GFRP specimens reached saturation shorty after exposure (within a few days) with comparable diffusion rates in all directions. The moisture content at saturation for all immersion scenarios was almost identical and close to 5%. However, exposure to high relative humidity (45 °C 95% RH) resulted in a negligible 0.2% moisture saturation content. This behaviour is believed to be due to the presence of mat layers that absorb liquid moisture. On the contrary, the CFRP specimens did not reach saturation in any of the exposure scenarios after one year of exposure. Figure 4.9 shows the experimental moisture uptake curves of GFRP and CFRP specimens conditioned at 45 °C DW. The considerably slower diffusion rate and moisture content at saturation of CFRP specimen indicates the negligible permeability of this material. Since both E-glass and carbon fibres are impermeable, the resin type, stack lay-up and production method can be the reason for this behaviour.

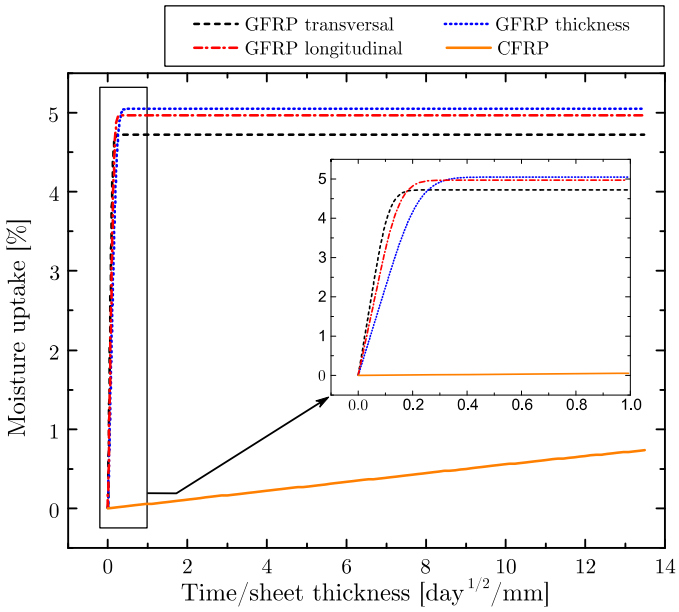

Figure 4.9. *Moisture uptake curves of FRP composites conditioned at 45 °C DW.*

4.3 Mechanical properties of adhesive

Tensile tests on dog-bone specimens were conducted to investigate the effects of moisture on mechanical properties of adhesive. In addition the effect of the following aspects was studied: (i) fast curing, (ii) salt water solutions, (iii) temperature as an accelerating factor and (iv) cyclic exposure conditions. The cyclic exposure tests are still ongoing and, thus, are not presented in this section. The specimens were manufactured in a Teflon mould according to ASTM D638-10 [132] with a thickness of 4 mm and dimensions marked on

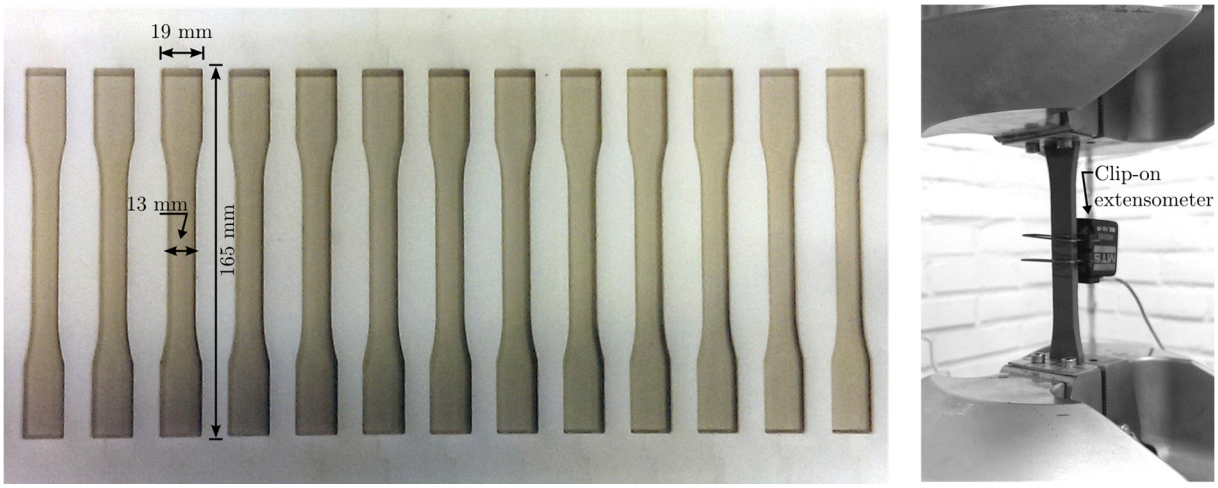

Figure 4.10. *Adhesive dog-bone specimens: (a) manufacturing mould; (b) test setup.*

Figure 4.10(a). After pouring the adhesive into the mould, a constant pressure was applied to remove the excessive adhesive and obtain a uniform thickness. Afterwards, the mould was placed in an oven at 60 °C for 48 hours for the case of fast cured specimens. The other specimens were cured at room temperature (RT cured) for one week. The pressure was maintained during the whole curing procedure. In total 50 specimens were manufactured, ten of which were tested directly in the dry state and the rest were exposed to the ageing conditions listed in Table 4.1. After nine months of exposure, the specimens were removed from the conditioning environment and tested to failure.

The quasi-static tests were performed in displacement control mode and at constant speed of 0.2 mm/min. A clip-on extensometer with a gauge length of 25 mm was used to measure the strains in the narrow section of the specimen, see Figure 4.10(b). Prior to the tensile tests, the geometry of all the specimens, namely thickness and width, was measured at three points in the narrow section of the specimen. The measured values were used to obtain an average thickness and width per specimen in order to calculate the axial stress. The test results of specimens with trapped air bubbles in the failure section were neglected. Nevertheless, a minimum of three specimens were included for each condition. Figure 4.11(a) shows the results obtained for the dry specimens. It can be seen that fast curing has led to a considerable drop in the stiffness compared to RT cured specimens. This observation has been witnessed in an earlier research [133], and is believed to be due to the formation of thermal residual stressed during the fast curing process.

In order to obtain the elastic modulus of tested adhesive specimens, the stress-strain curves were used. Firstly, a high order polynomial curve is fitted to the experimental results through non-linear curve fitting to diminish the noise-induced experimental scatter. Afterwards, the elastic modulus was calculated as the slope of the initial linear part of the curve between 0.05% and 0.2% strain values. Table 4.2 summarizes the test results in terms of elastic modulus, strength, and maximum strain, which were categorized based on the moisture content at the time of testing. The moisture contents were derived by means of 3D mass diffusion simulations in Abaqus® and are explained in Section 8.

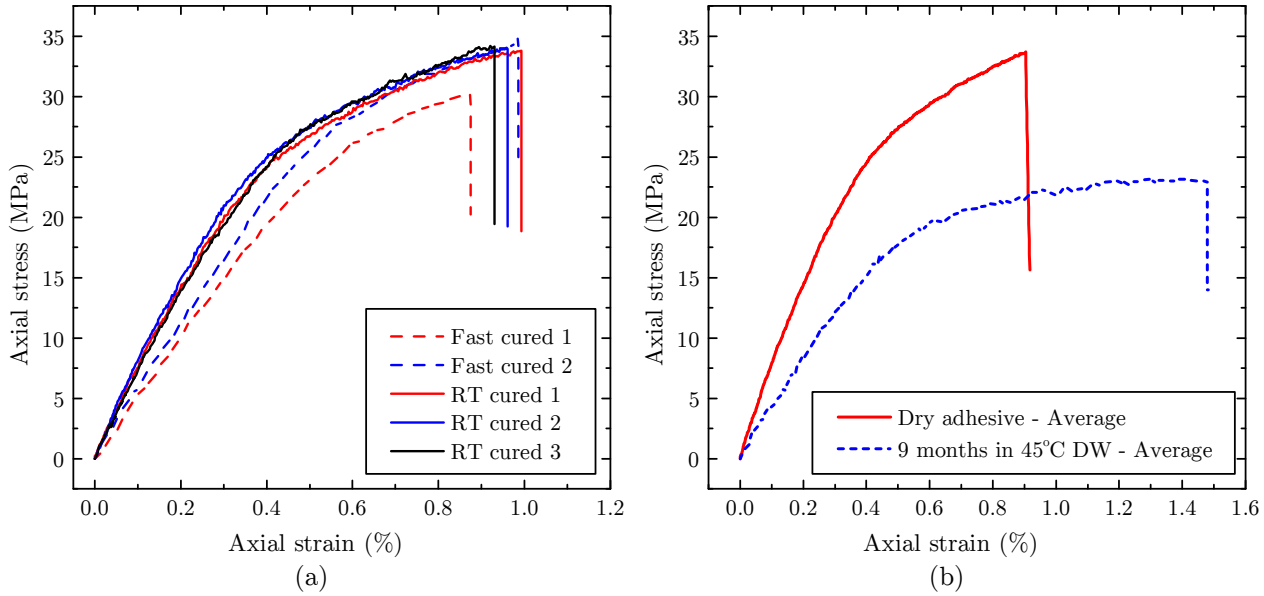

Figure 4.11. *Stress-strain curves of dog-bone adhesive specimens: (a) room temperature (RT) curing vs. fast curing of specimens; (b) dry vs. wet adhesive specimens.*

Table 4.2. *Experimental results of dog-bone adhesive specimens with varying moisture content.*

Ageing condition	Moisture content [%]	Elastic modulus [GPa]	Strength [MPa]	Max. strain [%]
Dry – RT cured	0	7.162	34.09	1.01
		7.056	33.78	0.98
		6.936	33.80	0.99
		7.267	34.04	0.96
		6.928	34.15	0.93
Dry – Fast cured	0	5.565	29.98	0.91
		5.146	30.17	0.87
		5.420	34.92	0.98
20 °C – Salt water	0.7807	5.663	20.35	1.16
		6.336	30.89	1.08
		6.021	30.05	1.10
20 °C – Distilled water	0.879	5.092	27.84	1.32
		5.372	28.79	1.41
		4.930	27.12	1.28
		5.601	-	-
45 °C – 95% RH	1.0976	4.260	27.16	0.91
		4.755	26.12	0.90
		4.355	25.32	0.94
45 °C – Salt water	1.3403	4.483	27.67	1.1
		4.775	27.29	1.23
		5.310	28.12	1.05
45 °C – Distilled water	1.476	3.655	23.34	1.39
		3.323	24.44	1.36
		4.111	23.24	1.45

The averaged stress-strain curves of specimens in the dry state and after nine–month of ageing in 45 DW condition are illustrated in Figure 4.11(b). A comparison of the two curves, clearly indicates the degradation of mechanical properties of adhesive caused by moisture. Nevertheless, with the failure strain increased by almost 40%, the aged adhesive exhibits more ductility.

The correlation between mechanical properties of adhesive and moisture content are plotted in Figure 4.12. Evidently, not only these properties have a strong dependency on moisture content, but also on the solution in which that level is achieved. In particular, the salt water solution appears to affect the mechanical properties less severe than distilled water. In order to develop a predictive equation for these properties as a function of moisture

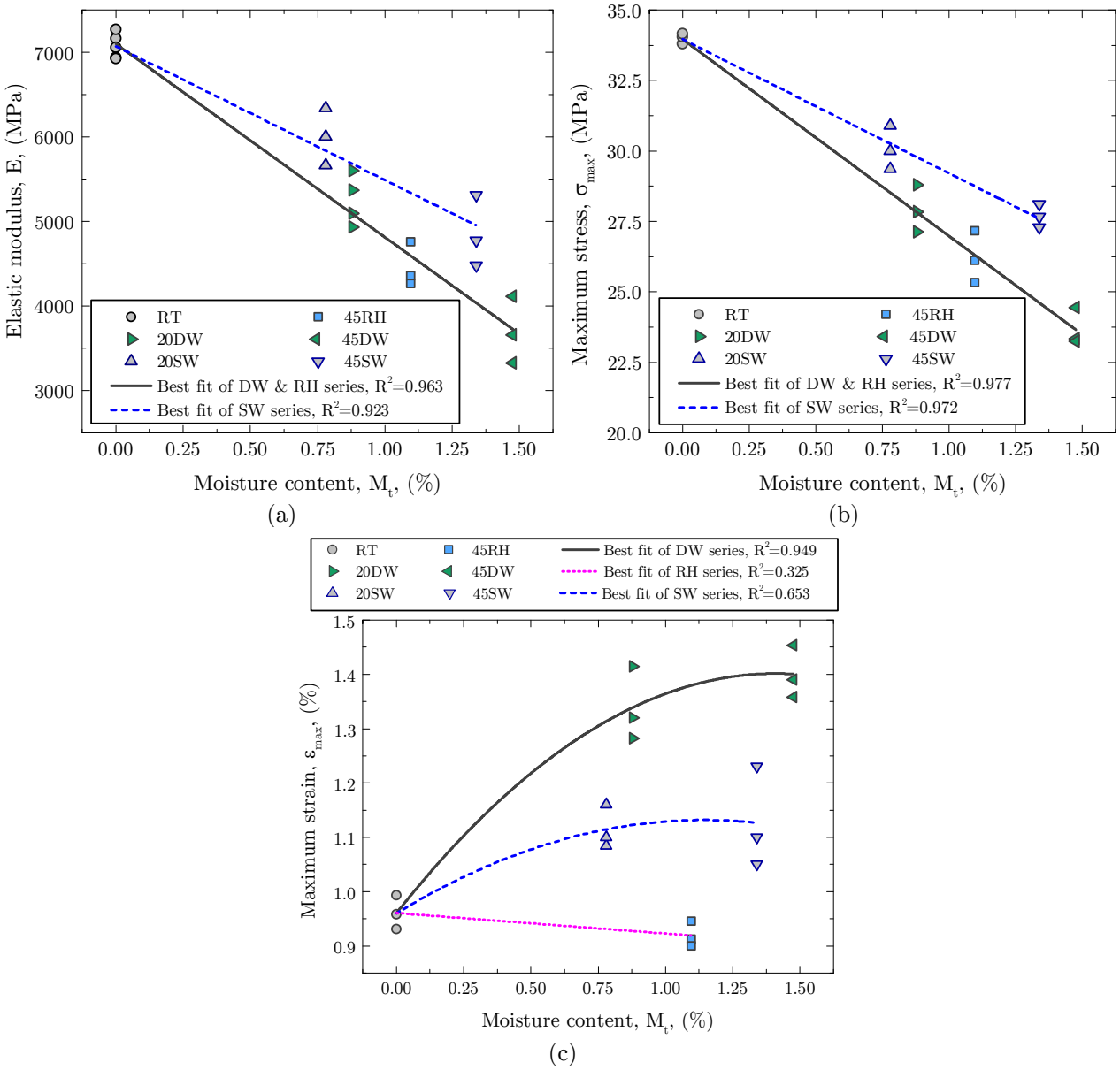

Figure 4.12. *The effect of moisture on mechanical properties of adhesive: (a) elastic modulus, (b) tensile strength, (c) strain at failure.*

content, non-linear curve fitting is conducted. As can be seen, the changes of tensile strength and elastic modulus can be predicted with good accuracy using a linear relationship. The obtained predictive equations for elastic modulus, E, and tensile strength, σ_{max}, as a function of moisture content, M_t, are as follows:

E-modulus in distilled water or vapour conditions:

$$E\ [MPa] = 7100 - 2287M_t\ [\%] \tag{4.1}$$

E-modulus in salt water:

$$E\ [MPa] = 7100 - 1607M_t\ [\%] \tag{4.2}$$

Tensile strength in distilled water or vapour conditions:

$$\sigma_{max}\ [MPa] = 34 - 6.98M_t\ [\%] \tag{4.3}$$

Tensile strength in salt water:

$$\sigma_{max}\ [MPa] = 34 - 4.75M_t\ [\%] \tag{4.4}$$

As Figure 4.12(c) indicates, the failure strain generally increases with moisture content. An exception is the failure strain of specimens exposed to vapour condition (95% RH) in which the failure strain slightly decreases. This observation reveals that ductility depends not only on the moisture content and conditioning solution, but also on the moisture state (vapour or liquid). For the immersion scenarios, the relationship of failure strain with moisture content is not linear. Hence, a parabolic equation is curve fitted to these series. The relatively low coefficient of determination, R^2, suggests a weaker correlation of this parameter with moisture content. This finding is in agreement with the reported results for various epoxy adhesives that are discussed in Paper I. However, the failure strain, ε_{max}, in moist conditions can be predicted by the following equations:

Failure strain in distilled water:

$$\varepsilon_{max} = 0.96 + 0.63M_t - 0.22M_t^2 \tag{4.5}$$

Failure strain in salt water:

$$\varepsilon_{max} = 0.96 + 0.3M_t - 0.13M_t^2 \tag{4.6}$$

Failure strain in high relative humidity levels:

$$\varepsilon_{max} = 0.96 - 0.038M_t \tag{4.7}$$

It is clear from the results presented in this section that there is a strong correlation between mechanical properties of adhesive and its moisture content. For adhesive specimens immersed in distilled water and 1.5% moisture content, the elastic modulus drops by more than 50%. Comparatively, the specimens with the same moisture content but immersed in salt water exhibit less deterioration with 33% reduction in elastic modulus. The degradation

of tensile strength is less severe and is around 30% and 20% for the same moisture content obtained in distilled water and salt water, respectively. As the time of exposure was kept constant for all specimens, the specimens exposed at 20 °C did not reach full saturation, and hence had a lower moisture content than the fully saturated specimens conditioned at 45 °C. However, the elastic modulus and tensile strength are shown to decrease linearly with the moisture content, irrespective of the temperature at which the materials were conditioned. This is consistent with the collected data of similar tests reported in Paper I for a wide range of epoxy adhesives, where a nearly linear drop of elastic modulus and strength with increasing moisture content is observed.

4.4 Mechanical properties of FRP materials

As it was discussed in Section 2.2.4, moisture can affect the mechanical properties of FRP composites. However, for unidirectional composites, moisture effects are more pronounced on resin-dominated properties, such as interlaminar shear strength, than fibre dominated properties, such as tensile strength. However, in order to account for probable changes in tensile strength and stiffness of the used FRP composites, this test series was included. Therefore, GFRP and CFRP tensile coupon specimens were prepared according to ASTM D3039/D3039M-14 [134]. The provided prefabricated laminates were cut into 25 × 250 [mm] (width × length) coupons using water-jet cutting technique. The thickness of the coupons was 10 and 1.25 mm for the GFRP and CFRP, respectively.

Table 4.3 summarizes the exposure conditions and testing plan for the tensile coupon tests. Tests are planned to be conducted after 6 months and 12 months of exposure. Two specimens of each kind will be tested at each occasion. In addition, to check the cyclic exposure performance, a series of specimens were removed from the exposure environment after six months and placed in an oven at 45 °C. The drying will be continued for an additional 6 months after which the tensile tests will be conducted. These tests are still ongoing, and thus the results are not included in this thesis.

Figure 4.13 depicts the FRP specimens exposed to the 45 °C 95% RH environment.

Table 4.3. *Exposure conditions and testing plan for the tensile coupon FRP specimens.*

Exposure environment			Testing plan	
Temperature	Humidity level	Solution	Testing interval [months]	Number of specimens
45 °C	Immersion	5% NaCl	6, 12	4
45 °C	Immersion/Drying	5% NaCl	12	2
45 °C	Immersion	Distilled Water	6, 12	4
45 °C	Immersion/Drying	Distilled Water	12	2
45 °C	95% Relative Humidity	Distilled Water	6, 12	4
45 °C	95% RH/Drying	Distilled Water	12	2
20 °C	Immersion	5% NaCl	6, 12	4
20 °C	Immersion	Distilled water	6, 12	4
20 °C	Room environment	--	0	3

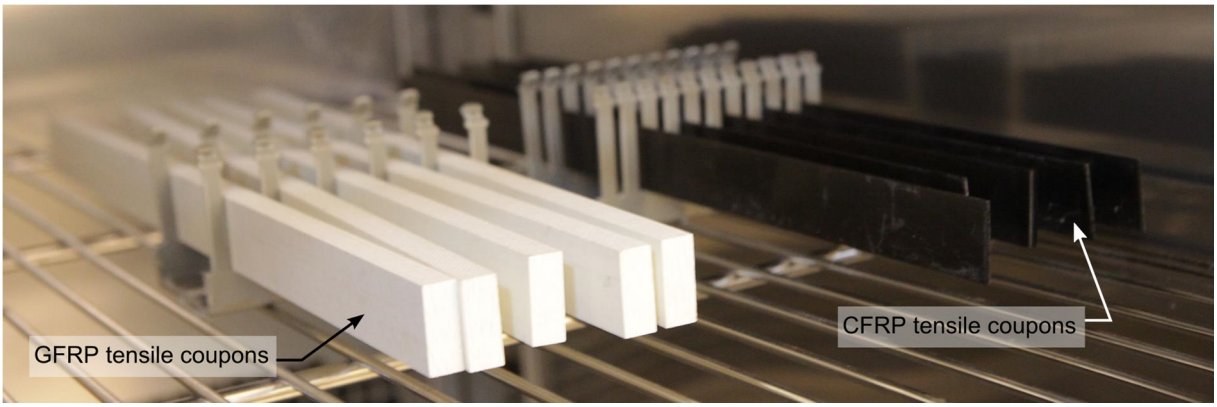

Figure 4.13. *FRP tensile coupon materials in the conditioning chamber at 45 °C 95% RH.*

4.5 Fracture toughness of adhesive/steel joints

It is generally accepted that the fracture mechanics approach is better capable to describe the mechanical rupture compared to the classical strength of material (stress-based) approaches. This is mainly due to the presence of singularities in the stress field of bonded assemblies which induces the stress-based design criteria to be fundamentally mesh-size dependent. However, a challenging and crucial perquisite of the fracture mechanics approach is to accurately characterize the fracture properties, such as the fracture energy.

The fracture toughness of the dry adhesive/steel joints loaded in peeling (mode I) and shear (mode II) had been previously characterized in [135,136]. Accordingly, double cantilever beam (DCB) and end notched flexure (ENF) configurations were employed. The results are presented and discussed in Paper II, where it is found that the utilized testing procedures and specimen configurations can yield accurate results. However, these configurations are not suitable for obtaining the moisture dependent properties of adhesive since only their bond-line edges are directly exposed to moisture. In other words, the moisture diffusion path to the centre of the joint becomes very long. As a result, an unreasonably long time is required before the entire bond-line experiences a uniform moisture uptake. In addition, even if the moisture distribution becomes uniform across the entire bond-line, yet the degradation would be non-uniform. This is because the adhesive with shorter moisture diffusion paths (outer region) gets saturated earlier than the inner regions with longer moisture diffusion paths. Consequently, the outer regions undergo longer moisture exposure durations (i.e. more damage) compared to the inner regions.

Open-faced specimens can be used to overcome the aforementioned disadvantages of standard fracture characterization configurations. These specimens are fabricated by applying the adhesive on one side of a single adherend to obtain a uniformly thick "primary bond" with a free surface to be exposed to moisture, see Figure 4.15. Hence, a more spatially uniform state of degradation can be achieved in a noticeably shorter time. After exposure of the open-faced specimen to a given environment, the open surface of the aged adhesive is bonded to another adherend using a "secondary" adhesive. This secondary adhesive should

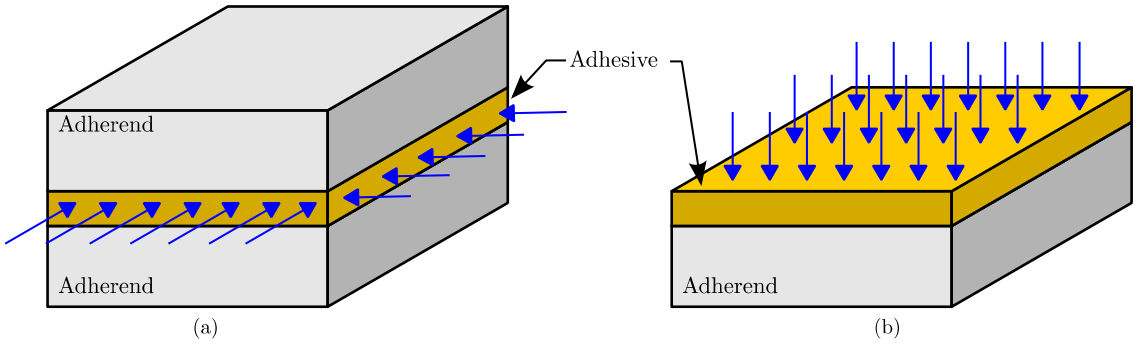

Figure 4.15. *Schematic representation of moisture diffusion: (a) standard geometry; (b) open-faced geometry.*

ideally cure very fast and be stronger than the primary adhesive. A complete open-faced double cantilever beam (ODCB) specimen is illustrated in Figure 4.14.

In this study, open-faced DCB and ENF specimens are planned to be used to characterize the effects of moisture on fracture toughness of the adhesive material. The test specimens have the same dimensions as previously tested dry DCB and ENF specimens. It is also planned to test ODCB and OENF specimens in the dry state to account for the effects of manufacturing method. The test and fabrication setup is currently being developed and the specimens will be manufactured afterwards.

The outcome of these test series will be used in the modelling work to predict the strength of aged bonded joints. Thanks to considerably reduced required time to saturation, more issues are planned to be investigated. This includes the influence of (i) moisture content, (ii) salt, (iii) temperature, (iv) wet/dry cycles, (v) freeze/dry-thaw cycles, (vi) freeze/wet-thaw cycles, and (vii) time-dependent moisture exposure.

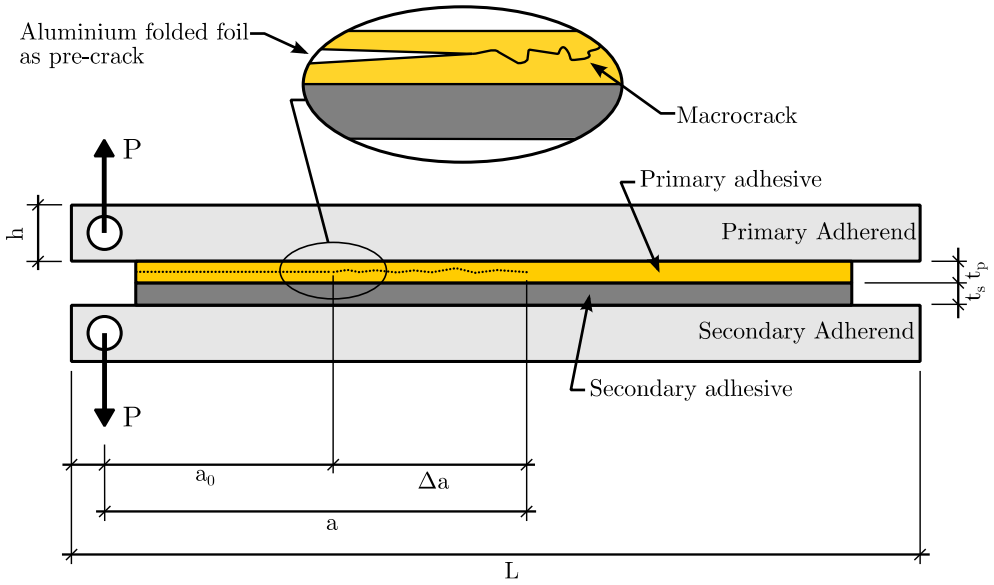

Figure 4.14. *The final configuration of an open-faced DCB specimen, after* [137] *(modified, not to scale).*

4.6 Fracture toughness of FRP/adhesive joints

The mode I and mode II fracture toughness of adhesively bonded joints composed of GFRP materials (supplied by the same manufacturer and with similar layup to the one used in this study) was recently investigated by Ye Zhang [138]. As shown in Figure 4.16(a) and (b), DCB and ELS (end loaded split) test configurations were used for mode I and mode II fracture characterization, respectively. The dominant failure mode, in both cases, was the fibre-tear failure in the mat layer of the GFRP laminate, Figure 4.16(c) and (d). This is mainly because the through thickness tensile and interlaminar shear strength of the laminate is lower than that of the FRP/adhesive interface.

As it will be discussed in Section 5, similar failure mode was observed for some of the FRP/steel bonded double lap shear joints tested in this study. Hence, the discussed configurations are suitable for investigating the influence of environmental factors on fracture of FRP composites in bonded joints. As the weak link in these joints is the FRP composite (adherend) which is in direct contact with moisture, the specimens can be manufactured using the traditional techniques, i.e. without open-faced fabrication method.

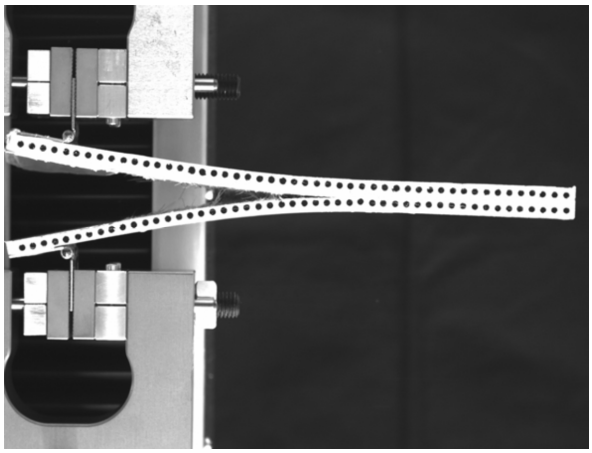

(a) DCB test setup

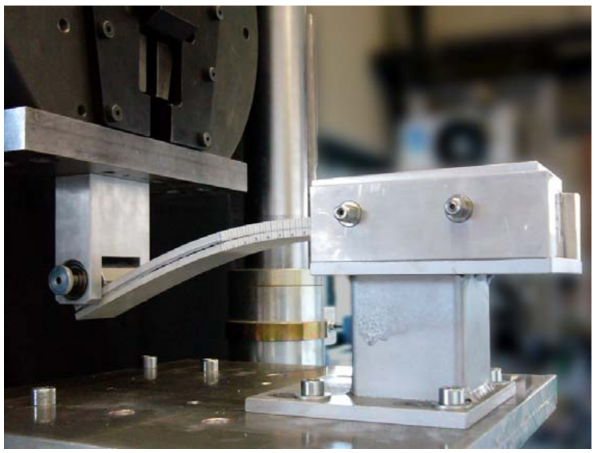

(b) ELS test setup

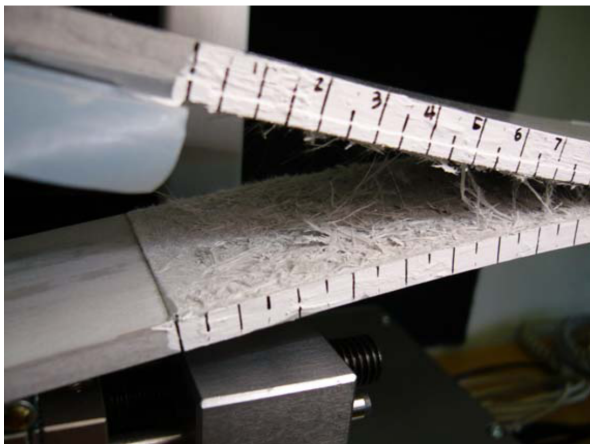

(c) Failure of DCB specimen in mat layer

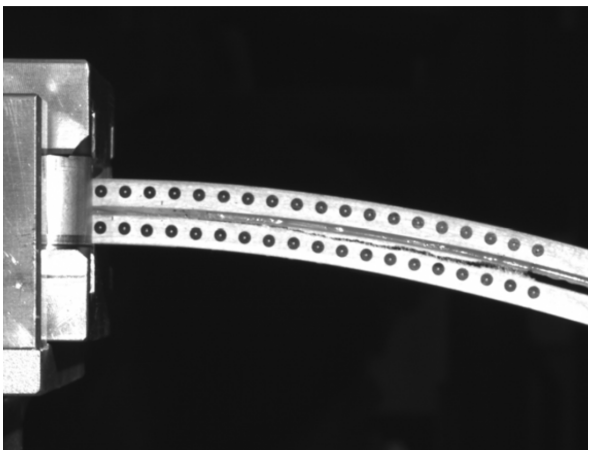

(d) Failure of ELS specimen in mat layer

Figure 4.16. *Test setups and failure modes of GFRP/epoxy joints for fracture characterization, after* [138].

The DCB configuration has been widely used to characterize the fracture under pure mode I loading. However, under pure mode II, the ENF and ELS configurations are commonly used. The ELS test allows more stable crack propagation and has been recently emerged as a valuable configuration. However, in contrast to the DCB specimen, no standard test dimensions exist for the ELS specimens. In fact, the definition of specimen dimensions depends largely on the adherends and adhesive properties. For the particular case of CFRP composite bonded joints, De Moura and Dourado [139] show that the ELS joints with dimensions marked in Figure 4.17(b) are appropriate. In addition, the authors suggest a data reduction scheme based on the equivalent crack method, ECM, which does not require the measurement of crack length during testing. Ye Zhang [138] also reports the good accuracy of the ECM method for the case of GFRP specimens.

In this context, the specimens depicted in Figure 4.17 will be used in this study.

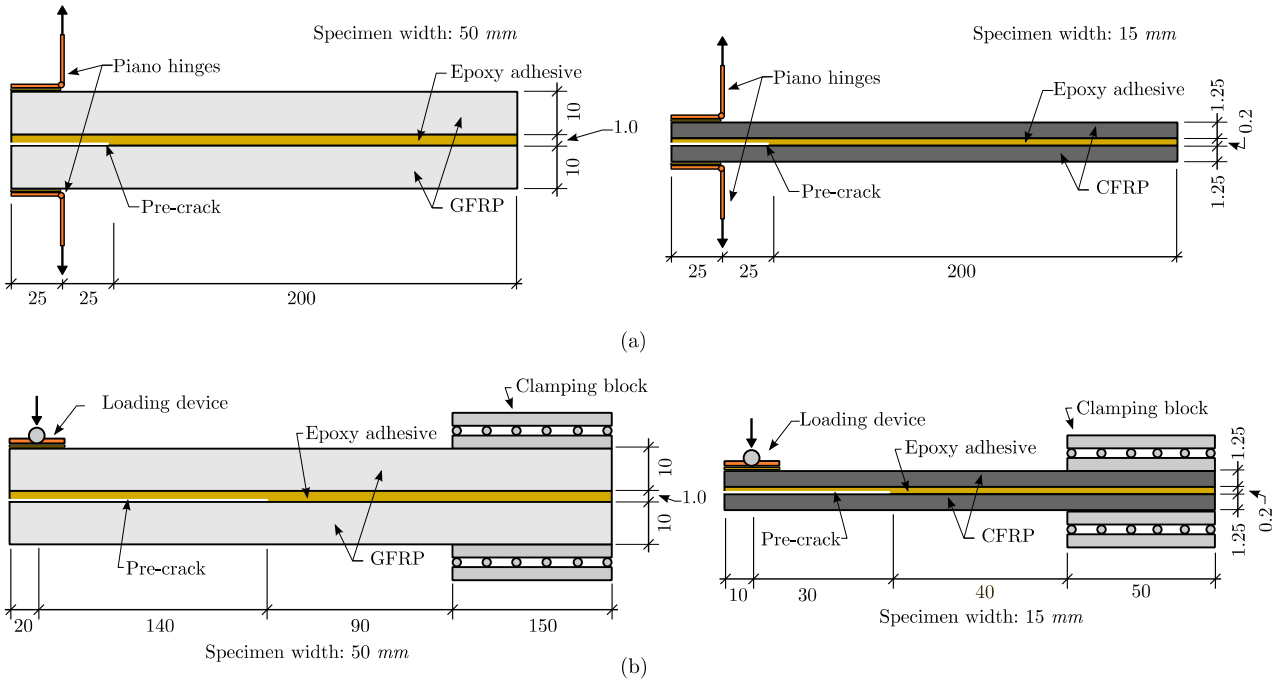

Figure 4.17. *Schematic representation of the fracture toughness tests for FRP/epoxy joints (dimensions in mm): (a) DCB configuration; (b) ELS configuration.*

5 Long-term durability tests of adhesively bonded FRP/steel joints

In order to investigate the long-term performance and identify the environmental damaging mechanisms at joint-level, adhesively bonded FRP/steel double lap shear (DLS) joints are manufactured. The advantage of this configuration compared to the other commonly used joints is the ease of failure detection and relatively straightforward testing procedure. In addition, the stress state at the outer ends of the bond line in a DLS specimen is very similar to that of steel girders strengthened with FRP laminates [140].

More importantly, this test series will be used to verify the FE analysis predictions of environmentally aged joints. Therefore, in the planning of the test matrix, special consideration was given to include sufficient testing intervals and exposure combinations.

5.1 Specimen configuration and manufacturing

Two types of DLS joints were designed: (i) with CFRP adherends (CDLS), (ii) with GFRP adherends (GDLS). The CDLS joints are intended to represent applications relating to strengthening of steel bridge girders, whereas the GDLS series represent GFRP bridge deck to steel girder connections. In both cases, the substrate is normal strength carbon steel (S355) and the used adhesive is STO® BPE lim 567. However, the thickness of the adhesive layer is 1.5 mm and 6.0 mm in CDLS and GDLS joints, respectively. The adhesive thickness was chosen to comply with typical bridge field joints for their intended application. In addition, the steel plates were chosen wider than the FRP laminates to resemble adhesive connections in bridges where the entire flange may not be covered by the FRP.

One of the most important aspect of manufacturing the DLS specimens is to achieve a proper bond quality. In this regard, the mechanical interlocking between the interfacial adhesive layer and steel was enhanced by augmenting the total exposed bond area of steel. This is achieved by sandblasting the steel surface to a degree equivalent to SA2$\frac{1}{2}$, as suggested in [5]. Afterwards, the steel plates were cleaned with high-pressure air and solvent (acetone) to remove the residual steel particles, dust and other contamination. The surface of both CFRP and GFRP laminates were roughened using fine sandpaper, cleaned with air pressure and rinsed with acetone prior to bonding. Finally, the DLS joints were manufactured using the specific moulding forms that were created for each specimen type, see Figure 5.1. To cure the adhesive layer, all the specimens were kept for at least seven days under room conditions.

The manufactured DLS joints are shown in Figure 5.2. As the adhesive bond in FRP deck to steel girder joints are usually away from the edges of the deck, moisture can only enter GFRP material from its surface. Therefore, the sides of some of the GDLS specimens were covered with a water-proof paint to represent filed applications, see Figure 5.2(c). Prior to

the exposure, all the specimens were marked, their dimensions were measured and documented, the bond-line edges were examined with a magnifying lens, and specimens with visible imperfections (such as micro cracks, trapped air pockets, adherends misalignments, etc.) were excluded.

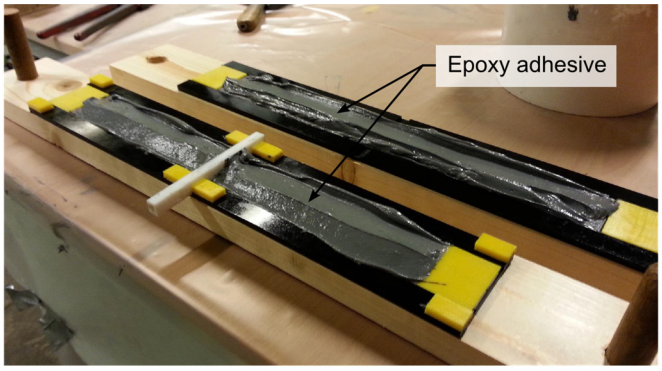

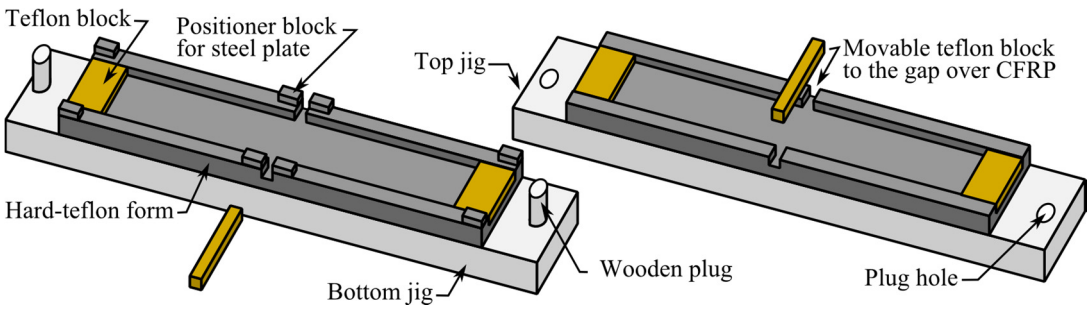

Figure 5.1. *Fabrication mould for DLS joints.*

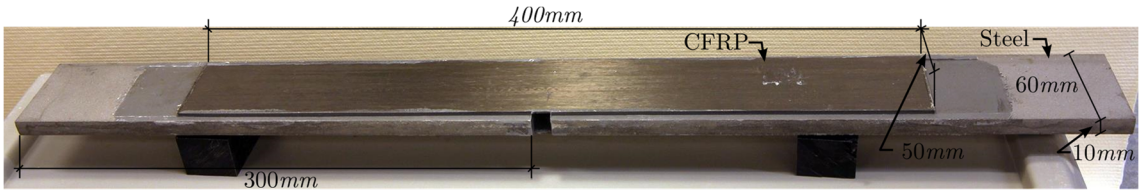

(a) DLS with CFRP adherends (CDLS)

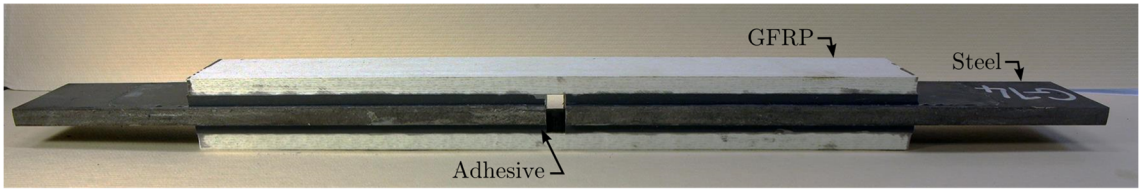

(b) DLS with GFRP adherends (GDLS)

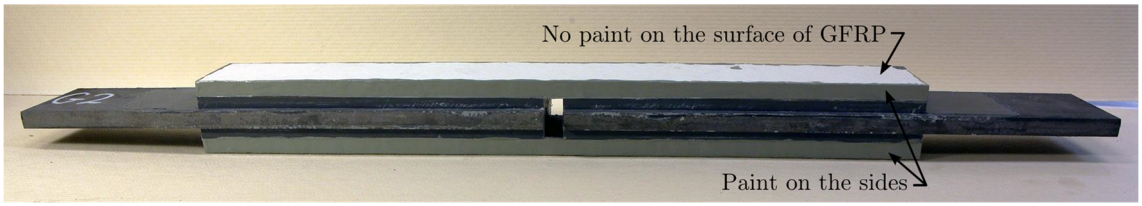

(b) DLS with side-painted GFRP adherends

Figure 5.2. *Manufactured DLS joints.*

5.2 Exposure scenarios

After the curing period, the manufactured DLS joints were exposed to a number of different exposure scenarios. The exposure conditions were planned according to the points discussed in Section 3.

In total, 120 DLS specimens were manufactured, of which 110 were exposed and 10 were tested in the dry-state as the control specimens. Table 5.1 lists the exposure matrix for the conditioned specimens. Two temperature regimes, namely 20 °C and 45 °C, were utilized to investigate the effects of increasing temperature on ageing mechanisms at joint-level. For each temperature, the specimens were immersed in distilled water or 5% NaCl solution. The salt solution concentration was chosen to represent de-icing salt solutions found in bridges, and is obtained by mixing 5% weight NaCl salt with distilled water. For the case of 45 °C, two special conditioning tanks were made by equipping high temperature resistant plastic boxes with submersible stainless steel electric heaters. In addition, each box is provided with two water circulating pumps to achieve uniform temperature distribution throughout the tank, see Figure 5.3(a). The exposure scenarios at 20 °C were conducted by placing similar water containers in a walk-in climate room with a constant temperature of 20 °C. All the containers were sealed and checked regularly.

In addition to constant immersion of specimens in the described conditions, cyclic exposure scenarios were performed. These scenarios include wet/dry and freeze/thaw cycles. The wet/dry condition was achieved by first immersing the specimens in water for a given time (four or eight months), followed by drying them at the same temperature and for the same duration. Moreover, after the drying cycle, some specimens were exposed to another wet cycle. The freeze/thaw condition was achieved by applying freeze/thaw cycles to specimens that had been immersed in salt- or distilled water at 45 °C for 18 months. The freeze/thaw cycles are being performed using an environmental chamber. Another series of specimens were exposed to outdoor conditions in Gothenburg, as depicted in Figure 5.3(b).

(a) (b)

Figure 5.3. *Exposure of DLS specimens: (a) heated-water tank, (b) outdoor conditions.*

Table 5.1. *Long-term exposure matrix of DLS joints*

Temperature	Exposure condition		Adherend	Exposure duration [months]	Quantity
45 °C	Distilled water (DW)	Constant immersion	CFRP	4	3
				6	3
				12	3
				18	2
		Cyclic wet/dry		8 (wet)	3
				8 (wet) / 8 (dry)	1
				8 (wet) / 8 (dry) / 8 (wet)	2
		Cyclic freeze/thaw (f/t)		18 (wet) / 50 [f/t cycles]	2
				18 (wet) / 100 [f/t cycles]	2
		Constant immersion	GFRP	2	2
				4	2
				6	2
				12	2
				18	2
	5% NaCl solution	Constant immersion	CFRP	4	3
				6	3
				12	3
				18	3
		Cyclic wet/dry		8 (wet)	3
				8 (wet) / 8 (dry)	1
				8 (wet) / 8 (dry) / 8 (wet)	2
		Cyclic freeze/thaw (f/t)		18 (wet) / 50 [f/t cycles]	3
				18 (wet) / 100 [f/t cycles]	3
				18 (wet) / 200 [f/t cycles]	3
		Constant immersion	GFRP	2	3
				4	3
				6	3
				12	3
				18	3
		Constant immersion	Painted GFRP	6	2
				12	2
				18	2
20 °C	DW	Constant immersion	CFRP	6	2
				12	2
	5% NaCl solution	Constant immersion	CFRP	4	3
				6	3
				12	3
		Cyclic wet/dry		4 (wet) / 4 (dry)	2
				4 (wet) / 4 (dry) / 4 (wet)	2
		Constant immersion	GFRP	6	3
				12	3
Outdoor conditions			CFRP	24	2
				48	2
				72	2
			GFRP	48	2

5.3 Test setup and Results

The DLS specimens were tested using an MTS universal testing machine with a capacity of 250 kN. The tests were performed in displacement control mode at a constant rate of 0.1 mm/min until failure. A series of LVDTs were used to measure the longitudinal and transverse deformation of specimens during testing. The test setup is shown in Figure 5.4.

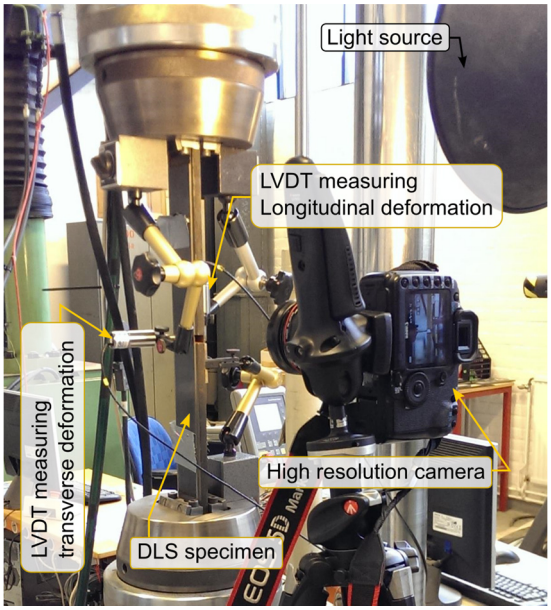

Figure 5.4. *Test setup of DLS specimens*

Due to the large number of specimens and the fact that some of the exposure scenarios were still ongoing, only the results of constant immersion conditions of CDLS specimens are reported in this thesis.

The failure of all the tested CDLS specimens initiated from the gap area. The crack initiation and failure mechanisms were recorded by means of a high resolution camera. In addition, the crack initiation load (failure load) and maximum load were distinguished, and are thoroughly discussed in Paper II.

The test results in terms of maximum load, maximum displacement and failure mode are listed in Table 5.2 for all the tested CDLS specimens. It can be seen that, for all the ageing conditions, with increasing exposure duration the failure mode shifts from cohesive failure in the adhesive layer to the interfacial or interlaminar failure, or a combination of both. However, the changes of load bearing capacity does not follow the same trend for all the cases, see Figure 5.6 and Table 5.3. Compared with the dry joints, the load-bearing capacity increases with exposure duration for the specimens immersed in both distilled- and salt water at 20 °C. After one year of exposure, the average load bearing capacity of these specimens increases by 10% and 15% for 20DW and 20SW series, respectively (see Figure 5.6(a) and (b)). Nevertheless, for the same exposure duration and irrespective of the solution type, the load-bearing capacities of the specimens aged at 45 °C gets reduced. In comparison with the dry joints, the reductions are ca. 9% and 25% for 45DW and 45SW series, respectively. It is interesting to note that, even in these series, exposure for shorter durations has led to increased load-bearing capacity. This critical period, during which the strength of the joint is not reduced, is eight months for the case of immersion in distilled water at 45 °C. Moreover, it can be seen from Table 5.2 that exceeding this critical time is accompanied by a change of failure mode from cohesive to interfacial failure. The critical time is found to be six months for specimens immersed in salt water at 45 °C.

Another observation from the test results, presented in Table 5.2, is a considerable reduction in the maximum longitudinal deformation of the joints as result of ageing. This is the

most pronounced for the joints immersed in salt water at 45 °C, in which the maximum displacement drops to less than 1.0 mm (compared to 1.9 mm for the case of dry joints) for the majority of the tested joints. This observation can be justified by the change of failure mode to interlaminar or interfacial failure.

The effect of ageing on stiffness of the joints is studied by plotting longitudinal deformation at different load levels vs. ageing time. These load levels are chosen to fall approximately before damage initiation, during damage development, and after crack imitation in the joint. The results are plotted in Figure 5.5. It can be seen that the joint stiffness is generally increased with increasing exposure duration (i.e. decreased displacement). Moreover, the stiffness gain is more pronounced at higher load levels. Given that the increased stiffness in only observed for the joints with interlaminar or interfacial failure mode, this observation

Table 5.2. *Test results of CDLS specimens in constant immersion conditions; DW: distilled water, SW: 5% NaCl salt water.*

Exposure condition	Exposure duration [days]	Maximum load [kN]	Max. longitudinal displacement [mm]	Failure mode
Dry	0	121.7	1.97	Cohesive
	0	121.8	1.93	Cohesive
	0	122.7	1.91	Cohesive
20°C DW	197	123.9	0.91	Interlaminar / interfacial
	197	135	1.09	Cohesive
	365	118.9	0.87	Interlaminar / interfacial
	365	149.9	1.27	Cohesive
20°C SW	197	132.2	1.29	Cohesive
	197	127.8	1.47	Cohesive
	365	140.5	1.08	Interlaminar / interfacial
	365	142.9	1.23	Cohesive
	365	139	1.07	Interlaminar / interfacial
45°C DW	119	123	1.65	Cohesive
	119	122.9	1.57	Cohesive
	243	127.1	1.97	Cohesive
	243	134.5	1.77	Cohesive
	243	124.7	1.71	Cohesive
	364	117.4	1.66	Interfacial / cohesive
	364	116.8	1.42	Interfacial / cohesive
	364	124.7	1.62	Interfacial / cohesive
45°C SW	120	111.5	0.69	Interlaminar
	120	121.1	1.08	Interlaminar
	120	128.2	1.21	Cohesive
	181	126.8	0.79	Interfacial
	181	121.1	0.73	Interfacial
	181	116	0.75	Interfacial
	239	98.5	0.73	Interlaminar / interfacial
	239	124	1.53	Cohesive
	239	103	0.76	Interlaminar
	364	113.6	0.91	Interfacial/cohesive
	364	79.9	0.87	Interlaminar
	364	111	1.25	Interfacial / cohesive

can be explained as follows: as a consequence of moisture ingression, the highly stressed adhesive close to the gap area gets softened. This causes the peak stresses to decrease, which in turn delays the crack initiation in the adhesive. As a result, the joints exhibit an apparent stiffness gain at higher load levels. However, for the specimens with cohesive failure, the joint's stiffness is governed by the stiffness of the adhesive layer which, as previously discussed in Section 4.3, deteriorates in the presence of moisture.

Figure 5.7 shows some examples of fractured CDLS specimens with different failure modes. As can be seen, the bonded steel surface is not corroded in any of the specimens.

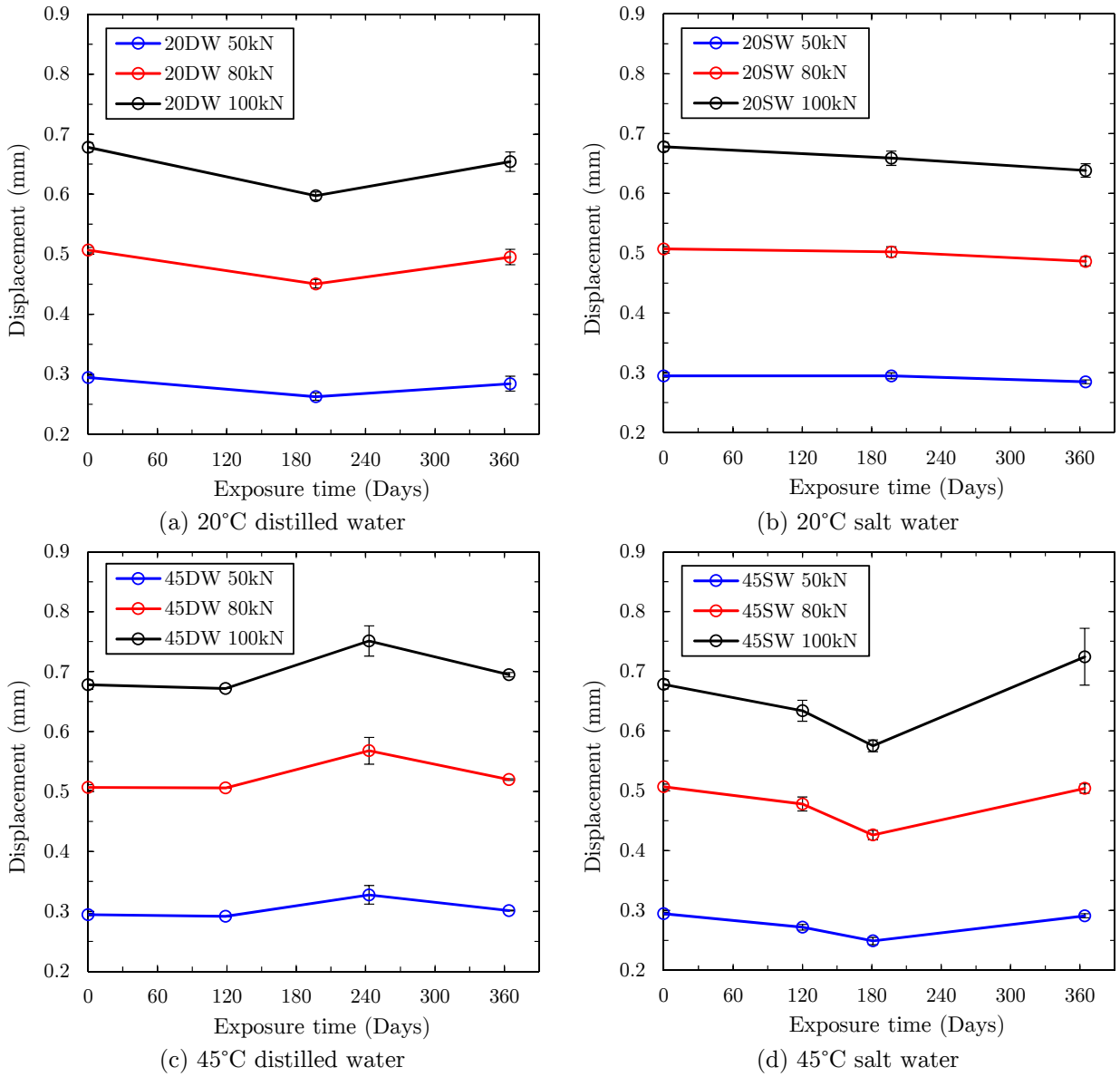

(a) 20°C distilled water (b) 20°C salt water

(c) 45°C distilled water (d) 45°C salt water

Figure 5.5. *Changes of longitudinal displacement at different load levels vs. exposure time of CDLS joints.*

Table 5.3. *Load bearing capacities of CDLS specimens in constant immersion conditions.*

Exposure condition	Exposure duration [days]	Average maximum load [kN]	Std. error	Average failure load [kN]	Std. error
Dry	0	122.07	0.3179	122.07	0.3179
20°C DW	197	129.46	5.5526	129.46	5.5526
	365	134.39	15.4837	134.39	15.4837
20°C SW	197	129.99	2.1789	129.99	2.1789
	365	140.82	1.1217	140.82	1.1217
45°C DW	119	122.97	0.0634	119.76	0.0601
	243	128.75	2.9596	128.75	2.9596
	364	119.66	2.5325	111.43	2.1681
45°C SW	120	120.27	4.8308	117.03	5.5778
	181	121.31	3.1332	121.31	3.1332
	239	108.50	7.8473	108.50	7.8473
	364	101.50	10.8359	91.36	6.7864

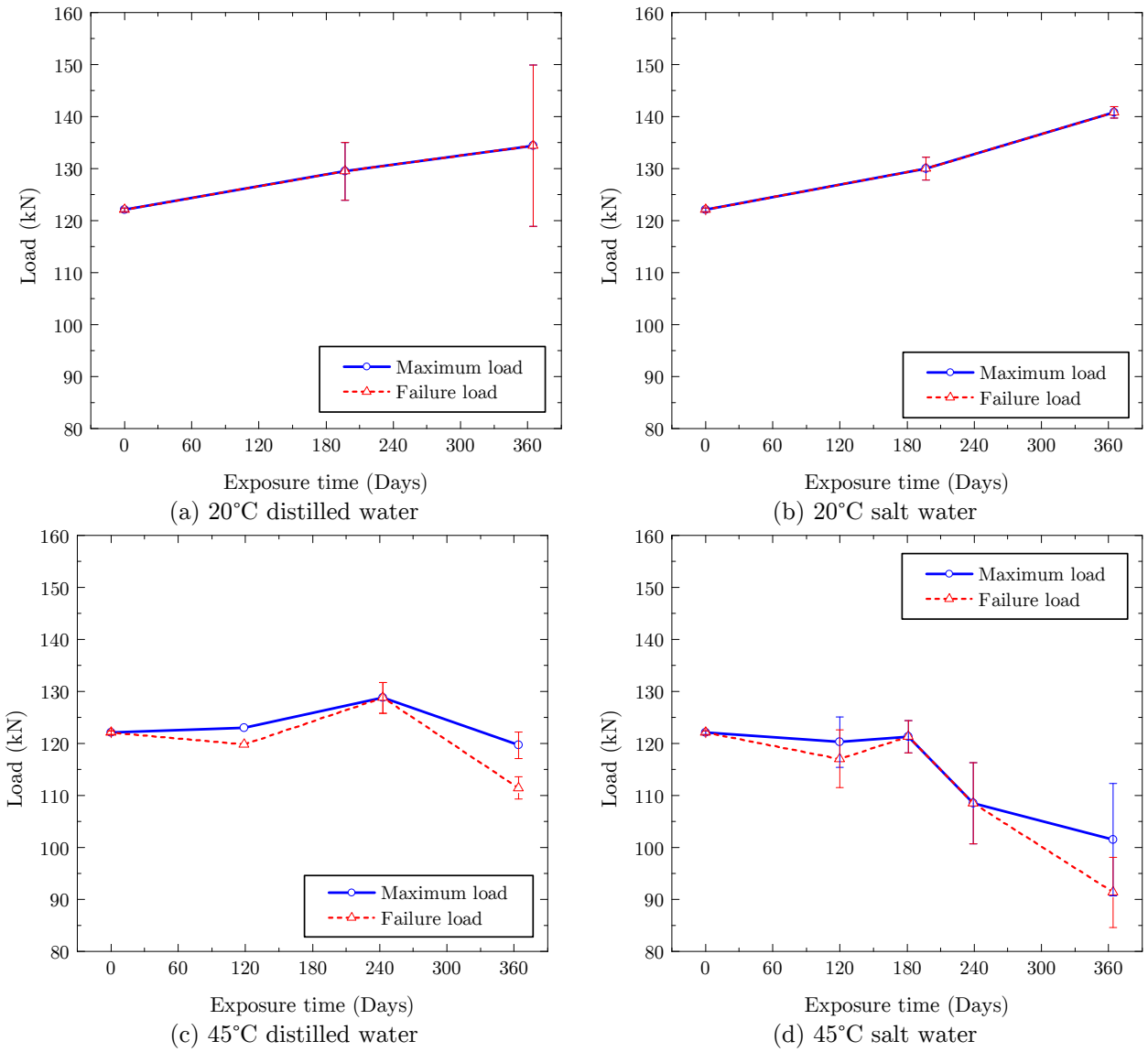

(a) 20°C distilled water

(b) 20°C salt water

(c) 45°C distilled water

(d) 45°C salt water

Figure 5.6. *Load bearing capacity vs. exposure time of CDLS joints.*

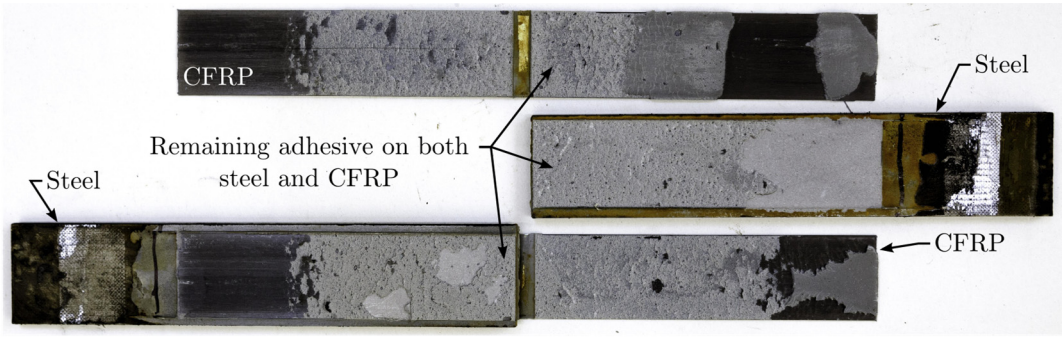

(a) Cohesive failure (specimen aged for 8 months in distilled water at 45°C)

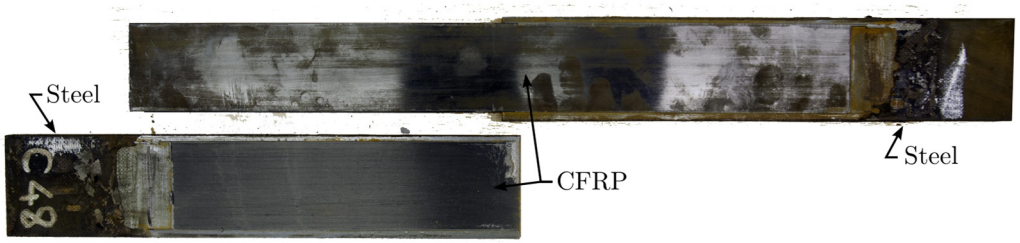

(b) Interlaminar failure (specimen aged for 2 months in salt water at 45°C)

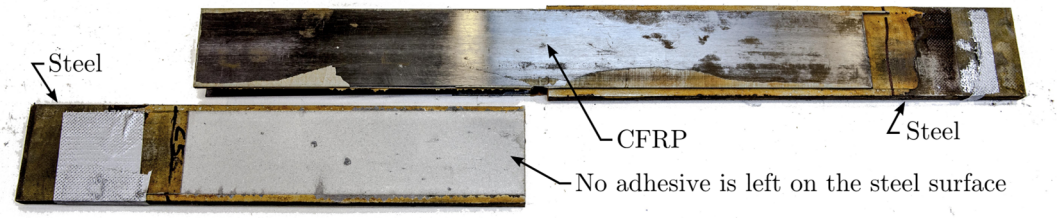

(c) Interfacial failure (specimen aged for 6 months in salt water at 45°C)

Figure 5.7. *Examples of different failure modes of tested CDLS specimens*

6 Overview of modelling scheme

The modelling scheme used to predict the performance of bonded FRP/steel joints is shown in Figure 6.1. As can be seen, the modelling approach is divided into three distinctive steps:

(1) static analysis to study the static response,
(2) mass diffusion analysis used to predict the moisture profile,
(3) cohesive zone modelling to predict the strength and fracture response.

As it is shown, the material input data for these models are obtained through the material characterization tests explained in Section 4. In this study, cohesive zone modelling is used to study the cracking and consequently failure of FRP/steel joints bonded with thick adhesive layer. As this numerical analysis model is intended to form the foundation of the damage mechanics based design approach, the effect of many parameters, such as the crack path location, adhesive thickness, and failure mode on the strength and mechanical response of the dry joints were investigated. Section 7 provides a short introduction to cohesive zone modelling and presents the key findings of the performed study. The complete results are reported in Paper II.

Moreover, mass diffusion and static analyses were sequentially coupled to study the effect of moisture on stress re-distribution in the adhesively bonded joints with permeable adherends. An introduction to these analyses, selected results as well as the key conclusions are given in Section 8, while an elaborate discussion is provided in Paper III.

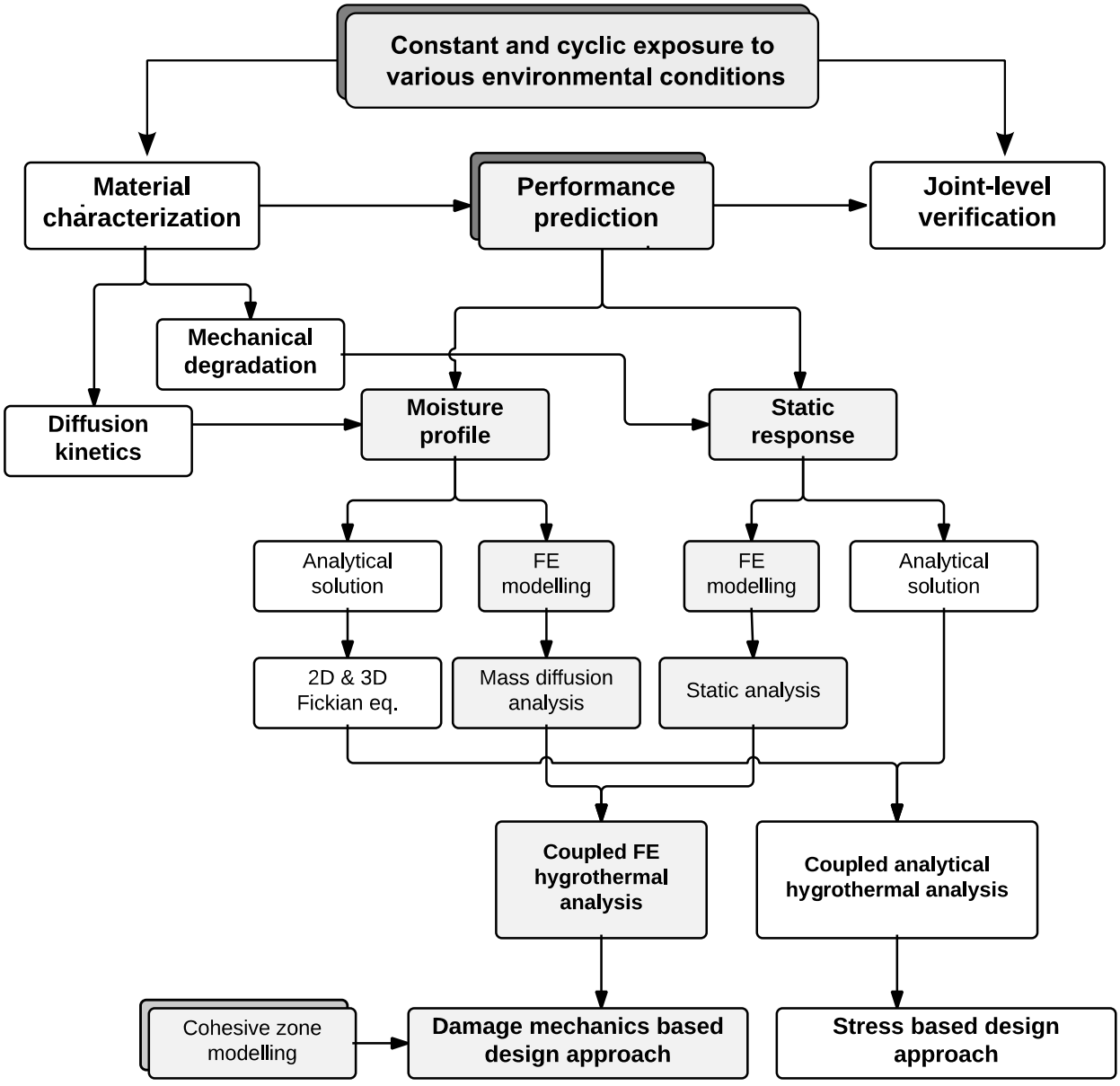

Figure 6.1. *Flowchart of the modelling scheme in this study.*

7 Failure prediction of adhesively bonded FRP/steel joints using cohesive zone modelling: Paper II

The design of steel/FRP adhesive joints is a complicated subject due to the variety of possible failure modes, including: (i) cohesive failure, (ii) debonding at steel/adhesive or FRP/adhesive interfaces and (iii) delamination in FRP. In addition, as it was discussed in Section 5.3, the failure of adhesive joints with a cohesive failure mode in the dry condition, often changes to interface failure mode after ageing. Therefore, to accurately analyse the failure of such joints, it is essential to consider approaches that are applicable to different failure modes.

Three major approaches can be used for failure analysis of bonded joints: (i) stress-based continuum mechanics, (ii) fracture mechanics-based, and (iii) damage mechanics-based approaches such as the cohesive zone modelling. The stress-based approaches suffer from the singularities at bi-material interfaces and sharp corners, and hence, cannot be used at the interfaces. The fracture mechanics-based approaches can be used to overcome the stress singularities at the interfaces. However, these methods assume an initial sharp crack which inevitably results in stress singularities at its tip. The damage mechanics approach, on the other hand, assumes a progressive damage before failure and, thus, is preferred.

Cohesive zone modelling (CZM) is an approach based on the damage mechanics-based modelling. CZM was first introduced by Barrenblatt [142,143] in 1959 to deal with the stress singularity at the sharp crack tip experienced in fracture mechanics analysis. In this approach, the fracture formation is considered as a gradual process in which the separation of the surfaces of the crack takes place across an extended crack tip, or cohesive zone, and is resisted by cohesive tractions, see Figure 7.1(a). As the two surfaces separate, the traction decreases. New crack surfaces are formed as the traction reaches zero. As depicted in Figure 7.1(b), this process is described by a cohesive law which relates the cohesive traction and relative separation of the cohesive zone surfaces.

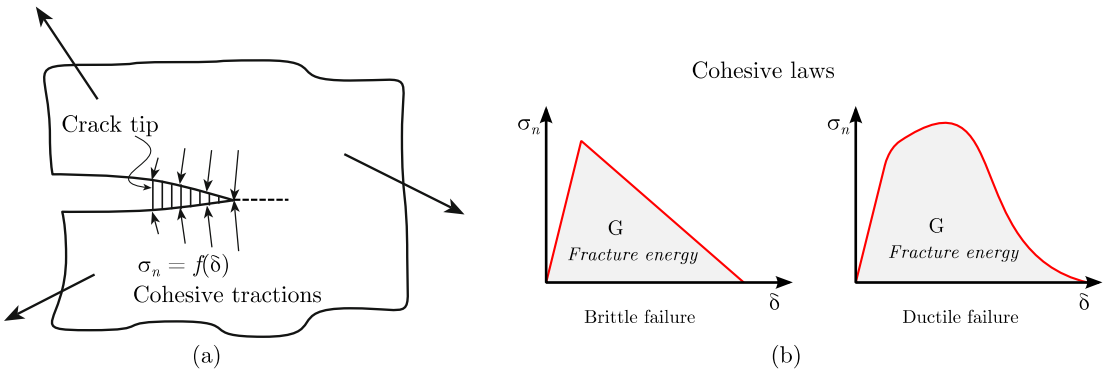

Figure 7.1. *(a) Schematic representation of cohesive zone at a crack tip, after* [141] *(slightly modified), (b) examples of cohesive laws for a brittle and ductile failure.*

Another advantage of CZM compared with the classical fracture mechanics approach is that it does not require an initial crack. This simplifies the modelling and calculations to a great extent. However, it is still necessary to define a crack path location. This becomes particularly important as the complexity of the joint increases. This is investigated in more details in Paper II, where it is shown that the location of the crack path in a single adhesive layer (at its centre or boundaries) does not have a significant effect on the predicted failure and mechanical behaviour. However, in joints with more than one adhesive bond, care should be taken with the placement of crack paths as this can lead to overestimations of the ultimate strength.

It is also shown in Paper II that the CZM approach can be successfully used to predict the damage process, ultimate strength and deformation of: (i) adhesively bonded CFRP/steel DLS joints with cohesive failure, and (ii) full-scale FRP-bonded steel beam specimens with interfacial failure. Furthermore, a combined interfacial/cohesive failure is also modelled. It is found that as long as the triggering failure mode remains cohesive in the adhesive, the combined interfacial/cohesive failure does not affect the ultimate joint strength. Nevertheless, maximum deformation is reduced significantly.

The CZM approach has been extensively used for failure analysis of adhesive joints used in many engineering fields [144–146]. However, comparably, the thickness of the adhesive layer in adhesive joints used in civil engineering applications are often several times larger. As can be seen in Figure 7.2, the thickness of the adhesive layer can affect the process zone in bonded assemblies. This is due to the appearance of an interface damage zone in the vicinity of the interface with adherends as the adhesive layer thickness decreases [147]. As a result, the fracture toughness can either get enhanced thorough stress shielding effect, or get exacerbated through the coalescence of voids before crack initiation. Given that the adhesive layer thickness is often disregarded in derivation of its fracture properties, its effect was investigated in Paper II by obtaining the cohesive law for thick adhesive layers. The derived parameters were implemented in failure analyses of DLS joints. It is found that neglecting the adhesive layer thickness can result in overestimation of the joint's strength. Nevertheless, for the studied DLS joint with an adhesive layer thickness of 1.5 mm, the difference in the predicted ultimate strength was negligible (ca. 5%).

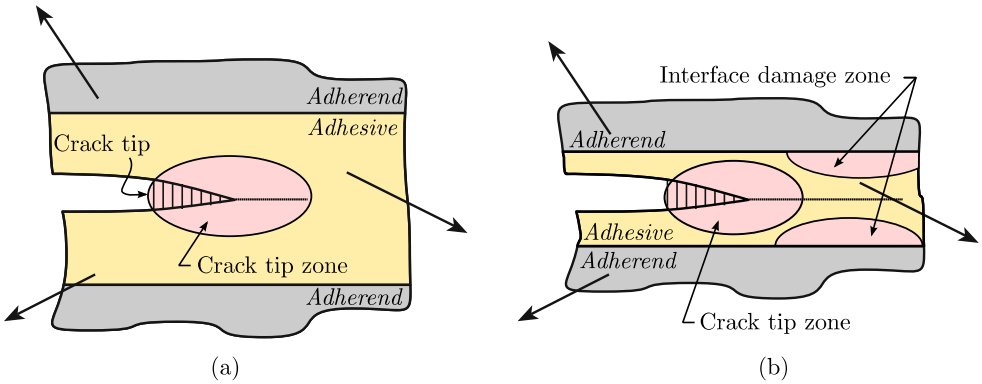

Figure 7.2. *Schematic representation of thickness effect on process zone of CZM in adhesive joints; (a) thick adhesive layer, (b) thin adhesive layer.*

8 Coupled diffusion-mechanical finite element analysis: Paper III

8.1 Mass diffusion analysis

Due to the analogy of the governing differential equations of heat transfer and Fickian diffusion, the classical heat transfer analysis is often used to simulate moisture diffusion into bonded assemblies. In this regard, moisture concentration and diffusivity are represented by temperature and heat conductivity, respectively. The basic assumption of heat transfer analyses is that the temperature profile, which could be considered as moisture concentration, has to be continuous across the thickness of the joint. Although this assumption is true in joints with impermeable adherends, it is violated when two or more permeable materials with different moisture saturation contents are bonded together. To resolve this problem, the heat transfer analysis can be replaced with mass diffusion analysis. In this context, the discontinuity problem is dealt with by using normalized concentration as the degree of freedom at the nodes. The normalized concentration is defined as the ratio of moisture concentration to moisture saturation content of each material.

In this study, 3D mass diffusion analyses were performed using the commercial FE analysis software Abaqus 6.13. Firstly, the gravimetric specimens were modelled using the Fickian diffusion parameters previously obtained in Section 4.2. This step is taken to verify the analysis, the used boundary conditions and modelling techniques, and is explained in paper III. Having verified the model, it was used to predict the moisture content of the dog-bone adhesive specimens after 9 month of exposure (at the time of tensile testing). Figure 8.1 shows a contour plot of moisture concentration (CONC) in the modelled assembly. Evidently, the specimen is not saturated after two months of immersion in salt-water at 45 °C.

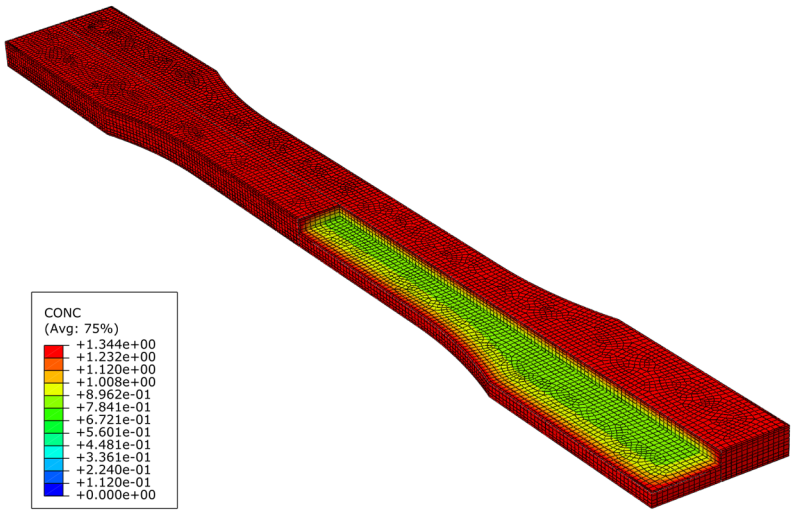

Figure 8.1. *Contour plot of moisture concentration profile in dog-bone epoxy adhesive specimen after exposure for 2 months to 45SW condition.*

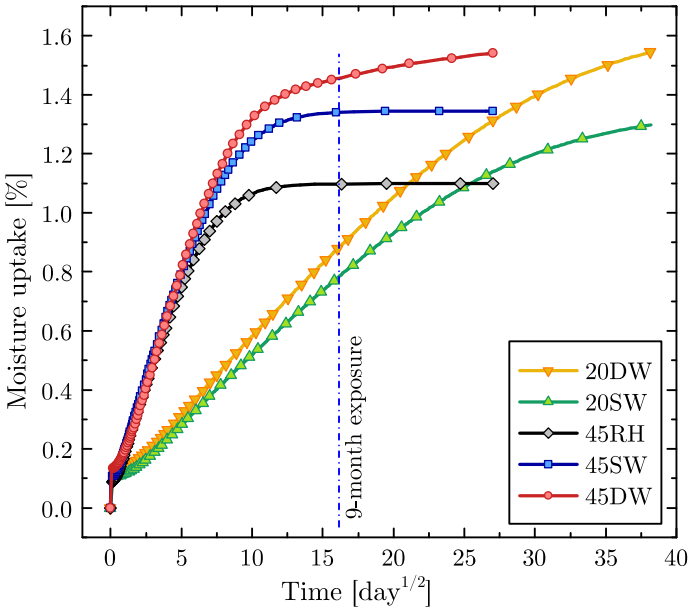

Figure 8.2. *Moisture uptake vs. exposure duration of the dog-bone adhesive specimens.*

The analysis results were post-processed to obtain the total moisture content of the specimens. The results are plotted in Figure 8.2 in which a vertical line is used to mark the 9-month exposure limit. Consequently, the corresponding moisture content of the specimens exposed to different ageing conditions were extracted. These values were used to analyse the test results of dog-bone specimens.

The moisture diffusion modelling of DLS joints is thoroughly discussed in Paper III. It is found that including the permeability of the adherends in moisture ingression analysis is crucial for accurate estimation of moisture profile in FRP/steel bonded joints. In addition, the efficiency of simple Fickian model over the dual-Fickian model is shown for joints with low permeability of adherends (such as the CFRP material used in this study). However, disregarding the relaxation dependent response of adhesive in joints with high permeable adherends can lead to underestimation of moisture content in the joint.

8.2 Sequentially coupled diffusion-mechanical analyses

Once the moisture profile in a joint is obtained, the elastic modulus of adhesive can be defined as a function of moisture content of each element. As a result, the effect of moisture on load transfer mechanism and stress redistribution at joint-level can be studied. In the modelling context, this was achieved by applying a pre-defined field variable of normalized moisture concentration in the adhesive material in the modelled DLS joint. The elastic modulus of adhesive was defined based on Equations 4.1 and 4.2. Therefore, the correct elastic modulus was attributed to each element automatically. Figure 8.3 shows the modelled geometry of the CDLS specimen. Only one quarter of specimen is modelled due to its symmetry. The stress redistribution in joints exposed to distilled water for up to 50 years are presented in paper III. Herein, the stress redistribution in a CDLS joint exposed to 45SW condition for 10 years are presented.

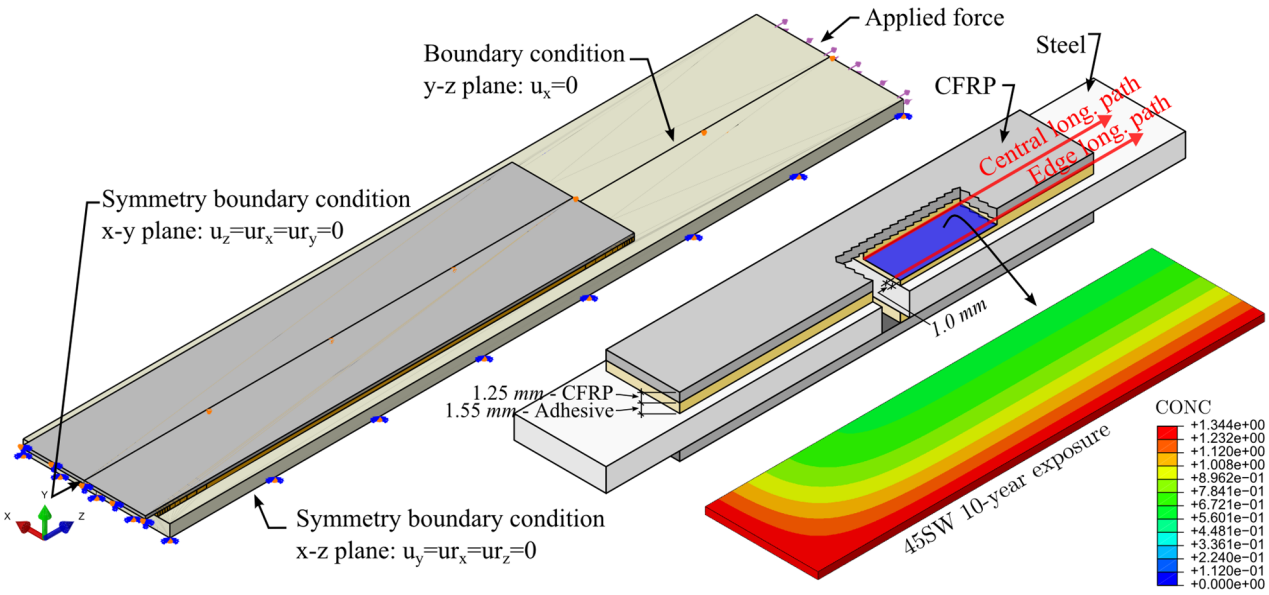

Figure 8.3. *Schematic representation of CDLS specimen (not to scale), modelled geometry and moisture concentration profile after exposure to 45SW for 10 years.*

The moisture concentration profile in the adhesive mid-layer after exposure to 45SW condition for 10 years is plotted in Figure 8.3. Only one quarter of the adhesive is shown due to its symmetry. As can be seen, the adhesive layer is not saturated after the 10-year exposure simulation period. Plots of stress distribution along the longitudinal paths and in the adhesive mid-layer are shown in Figure 8.4. The stresses are plotted for both the dry and "45SW 10-year" conditions. All the stresses are normalized with respect to the maximum principal stress along the edge path in the dry condition. As can be seen, the maximum principal stresses are the largest close to the gap which confirms the crack initiation location observed during experiments. Furthermore, the stresses are generally larger along the edge path compared with the central path. This is mainly due to the load transfer mechanism from the steel plates to the CFRP close to the gap location.

In comparison with the dry condition, the peak stresses have reduced after the 10-year exposure period. Moreover, since the adhesive close to the edge is almost saturated, the reduction is larger for the stresses along the edge path. Compared with the dry condition, the drop in the peak maximum principal stress is 12% and 16% along the central and edge longitudinal paths, respectively. It can be also seen from the plots of shear stress that the stresses are distributed along a larger area after exposure. Although very negligible, it highlights an increase in the anchorage length upon moisture ingression. However, as it was shown in Section 5.3 for joints exposed to 45SW condition, not only the strength is not increased, but also it has reduced after one year of exposure. This observation is discussed in Paper III. It is speculated that the presence of moisture for more than a critical time, can degrade adhesive/steel interface or FRP composite. Since the failure is governed by the weakest element, the drop in the peak stress does not lead to strength improvements in the joint.

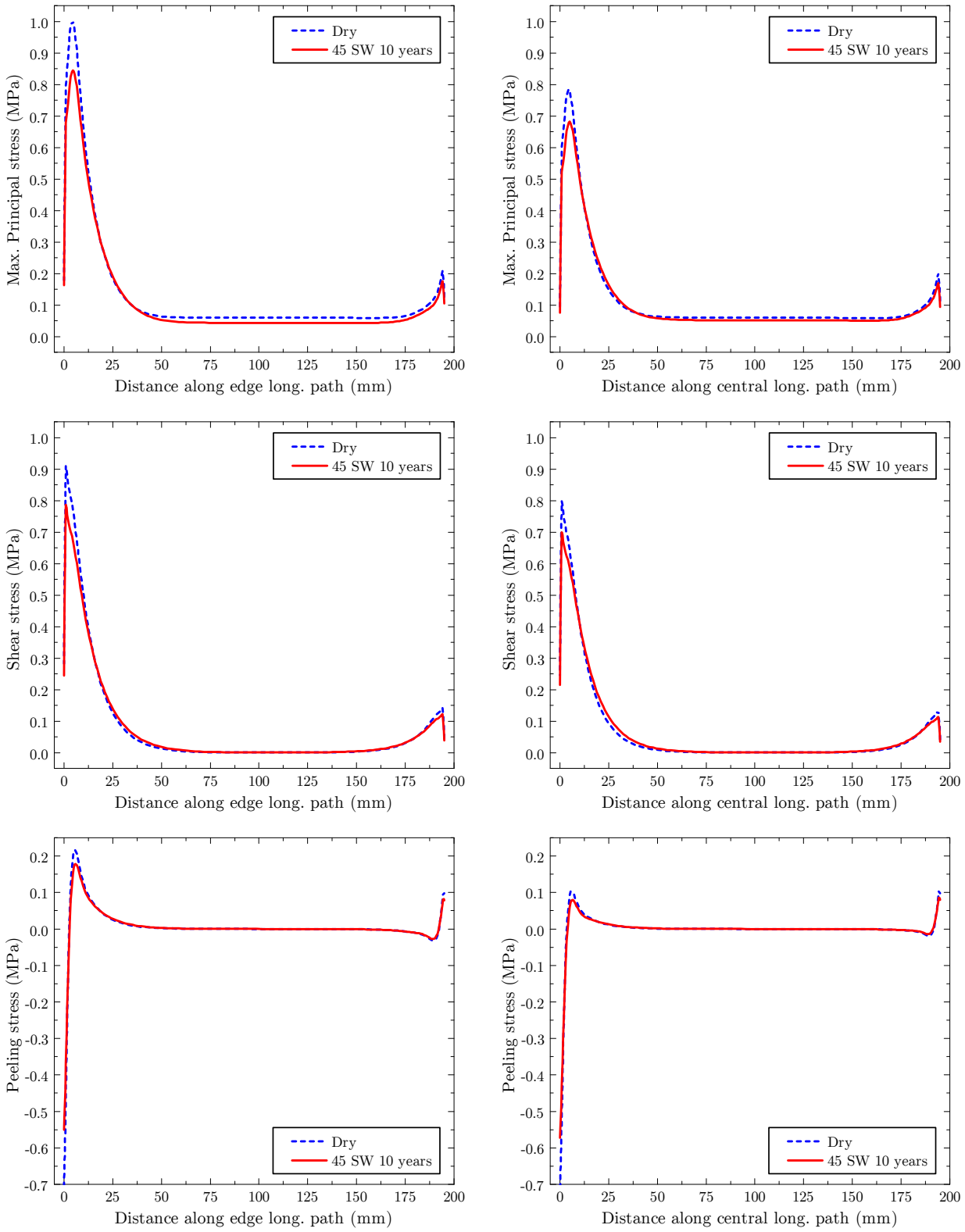

(a) along edge longitudinal path (b) along central longitudinal path

Figure 8.4. *Plots of stress distribution along the longitudinal paths shown in Figure 8.3; all values are normalized with respect to the maximum principal stress along the edge line in the dry condition.*

9 Conclusions

9.1 General conclusions

The aim of this study was to establish a framework for long-term performance and durability analysis of adhesively bonded FRP/steel joints in civil engineering applications. The state-of-the-art on durability aspects of FRP composites, epoxy adhesives and FRP/steel bonded joints in bridge applications were reviewed, and presented in Paper I. From this review, hygrothermal ageing (combination of moisture and temperature) was identified as the most influential factor on long-term performance of bonded joints in steel structures. In addition, a direct correlation between moisture content and mechanical degradation was identified. The literature review provided a framework to investigate the areas that remain unclear and need further research. Subsequently, a methodology including both experimental and numerical approaches was developed.

From the literature review, it was found that the failure mode of bonded joints generally changes after ageing. To accurately analyse the behaviour of joints with varying failure mode, cohesive zone modelling (CZM) was used. The CZM approach was found to be able to accurately predict the behaviour of FRP/steel joints used in bridges with interfacial, cohesive, and combined interfacial/cohesive failure modes. The distribution of crack paths in joints with more than one adhesive bond was found to significantly affect the post-fracture behaviour and ultimate strength of the joints. Moreover, it was suggested to take account of adhesive layer thickness in the derivation of cohesive-law parameters for the adhesive.

The effect of moisture on FRP/steel bonded joints was investigated by, firstly, characterizing the moisture diffusion into epoxy adhesive, GFRP, and CFRP materials that are used in bridge applications. This was achieved by conducting gravimetric measurements on specimens exposed to five ageing conditions. These conditions were designed to address the effects of temperature, humidity level, and de-icing salt solutions. It was found that the classical Fickian diffusion equation generally gives a good fit to the experimental results. For the epoxy adhesive specimens, the moisture diffusion rate was found to be a function of temperature, whereas the saturation content was governed by the humidity level or solution type. Furthermore, fast curing of the adhesive was found to have no significant effect on diffusion properties of fully cured epoxy specimens. Cyclic exposure of adhesive specimens to wet/dry conditions revealed a subtle raise in the moisture saturation content as the exposure cycles increased.

Due to the orthotropic structure of the GFRP material, its three-dimensional diffusion parameters were characterized by obtaining separate diffusion properties in each direction. Very similar diffusion behaviour was observed in all three directions irrespective of the ageing condition. The moisture saturation content of all the tested GFRP specimens was found to be strongly dependent on the humidity level; ca. 5% for immersion scenarios vs.

0.2% for the high relative humidity condition. Unlike the GFRP specimens, very slow moisture diffusion rate was observed for the CFRP material. Not only were none of the exposed gravimetric CFRP specimens saturated after one year, but also the absorbed moisture was found to be comparably negligible. Hence, the CFRP material was found to be almost impermeable.

The effect of moisture on mechanical properties of adhesive, as the weak link in bonded joints, was investigated by testing dog-bone specimens. The elastic modulus and tensile strength were found to decrease linearly with increasing moisture content. The reduction was more severe for the case of distilled water compared with salt water exposure conditions. The strain at failure was found to increase for immersed specimens, while it slightly decreased for those exposed to high relative humidity conditions.

The characterized moisture diffusion as well as moisture dependent mechanical properties of the FRP and adhesive materials were implemented in a coupled diffusion-mechanical FE model. This model was used to investigate the effects of moisture on load transfer mechanisms and stress distribution in adhesively bonded FRP/steel DLS joints. From the analyses results, including the adherends permeability was found to be crucial in moisture ingression analysis of bonded composite joints. In addition, simple Fickian was shown to be more time-efficient than the dual-Fickian model for joints with low adherent permeability. Due to the plasticized epoxy adhesive at the stress concentration zones, the peak stresses decreased continuously with increasing exposure duration. The anchorage length, on the other hand, was extended as the exposure continued.

From the tests on DLS joints after one year of hygrothermal exposure, the failure mode was found to change from cohesive failure in the adhesive layer to interfacial or interlaminar failure, or a combination of both. For all the exposure scenarios, an initial increase in the load-bearing capacity was observed during the first six months. However, the failure load of specimens aged at 45 °C reduced by 9% and 25% after immersion for one year in distilled and salt water, respectively. It is anticipated that the presence of moisture at the interface of steel/adhesive for a critical time can cause localized interfacial damage even at low moisture concentrations. However, at shorter exposure durations, moisture has a beneficial effect on the strength of the joint. Although negligible, ageing seemed to increase the stiffness of the joints. The stiffness gain was found to be more pronounced at load levels close to crack initiation.

9.2 Suggestions for future research

The following steps are suggested for the future research:

- Qualitative and quantitative characterization of the degradation of fracture properties of adhesive/steel interface and interlaminar fracture of FRP composites in the presence of moisture.
- Identification of the damage mechanisms and degradation level of bonded joint exposed to cyclic exposure conditions.
- Comparison of the degradation of FRP/steel bonded joints exposed to sub-zero and freeze/thaw cycles with and without moisture content.
- Implementation of the moisture dependent fracture properties of different components of FRP/steel bonded joints in the developed coupled FE model.

References

[1] Bell B. European railway bridge demography. doc no. d1. 2, sustainable bridges–assessment for future traffic demands and longer lives. Sixth Framew Program Eur Comm 2004.

[2] Karbhari VM, Shulley SB. Use of Composites for Rehabilitation of Steel Structures—Determination of Bond Durability. J Mater Civ Eng 1995;7:239–45.

[3] Bakis CE, Bank LC, Brown VL, Cosenza E, Davalos JF, Lesko JJ, et al. Fiber-Reinforced Polymer Composites for Construction—State-of-the-Art Review. J Compos Constr 2002;6:73–87.

[4] Hollaway LC. A review of the present and future utilisation of FRP composites in the civil infrastructure with reference to their important in-service properties. Constr Build Mater 2010;24:2419–45.

[5] Cadei JMC, Stratford TJ, Hollaway LC, Duckett WG. Strengthening metallic structures using externally bonded fibre- reinforced polymers 2004;44:174–80.

[6] Zhao X-L, Zhang L. State-of-the-art review on FRP strengthened steel structures. Eng Struct 2007;29:1808–23.

[7] Al-Emrani M, Haghani R, Kliger R, Crocetti R. Strengthening glulam beams with steel and composite plates. Proc. 7th Int. Conf. Compos. Sci. Technol. Sharjah, UAE, 2009.

[8] André A, Kliger R, Olsson R. Compression failure mechanism in small-scale wood specimens reinforced with CFRP: An experimental study. Constr Build Mater 2013;41:790–800.

[9] CNR-DT 202/2005. Guidelines for the Design and Construction of Externally Bonded FRP Systems for Strengthening Existing Structures, Metallic structures. Natl Res Counc Advis Comm Tech Recomm Constr 2007.

[10] Baldan A. Adhesively-bonded joints and repairs in metallic alloys, polymers and composite materials: Adhesives, adhesion theories and surface pretreatment. J Mater Sci 2004;39:1–49.

[11] Baldan A. Adhesively-bonded joints in metallic alloys, polymers and composite materials: Mechanical and environmental durability performance. J Mater Sci 2004;39:4729–97.

[12] Banea MD, da Silva LFM. Adhesively bonded joints in composite materials: an overview. Proc Inst Mech Eng Part L J Mater Des Appl 2009;223:1–18.

[13] Crocombe A. Durability modelling concepts and tools for the cohesive environmental degradation of bonded structures. Int J Adhes Adhes 1997;17.

[14] Da Silva LFM, das Neves PJC, Adams RD, Spelt JK. Analytical models of adhesively bonded joints—Part I: Literature survey. Int J Adhes Adhes 2009;29:319–30.

[15] Jain R, Lee L. Fiber Reinforced Polymer (FRP) Composites for Infrastructure Applications. 2012.

[16] Karbhari V, Chin J. Durability gap analysis for fiber-reinforced polymer composites in civil infrastructure. ... Compos ... 2003:238–47.

[17] Davis GD, Venables JD, Kinloch AJ. Durability of Structural Adhesives. Ed Kinloch, AJ, Appl Sci Publ, London 1983:43.

[18] Comyn J. Polymer permeability. Springer; 1985.

[19] Comyn J. Kinetics and mechanism of environmental attak. Durab. Struct. Adhes., Applied science publishers; 1983, p. 85–131.

[20] Pizzi A, Mittal KL. Handbook of adhesive technology, revised and expanded. CRC Press; 2003.

[21] Knox E., Cowling M. Durability aspects of adhesively bonded thick adherend lap shear joints. Int J Adhes Adhes 2000;20:323–31.

[22] Bowditch MR. The durability of adhesive joints in the presence of water. Int J Adhes Adhes 1996;16:73–9.

[23] Gledhill RA, Kinloch AJ, Shaw SJ. A Model for Predicting Joint Durability. J Adhes 1980;11:3–15.
[24] Karbhari VM. Durability of composites for civil structural applications. Woodhead Pub.; 2007.
[25] Chin JW, Nguyen T, Aouadl K. Effects of environmental exposure on fiber-reinforced plastic (FRP) materials used in construction. J Compos Technol Res 1997;19:205–13.
[26] Böer P, Holliday L, Kang TH-K. Independent environmental effects on durability of fiber-reinforced polymer wraps in civil applications: A review. Constr Build Mater 2013;48:360–70.
[27] Zhou J, Lucas JP. Hygrothermal effects of epoxy resin. Part I: the nature of water in epoxy. Polymer (Guildf) 1999;40:5505–12.
[28] Zhou J, Lucas JP. Hygrothermal effects of epoxy resin. Part II: variations of glass transition temperature. Polymer (Guildf) 1999;40:5513–22.
[29] Abanilla MA, Li Y, Karbhari VM. Durability characterization of wet layup graphite/epoxy composites used in external strengthening. Compos Part B Eng 2005;37:200–12.
[30] Zafar a., Bertocco F, Schjødt-Thomsen J, Rauhe JC. Investigation of the long term effects of moisture on carbon fibre and epoxy matrix composites. Compos Sci Technol 2012;72:656–66.
[31] Ashcroft I., Wahab MMA, Crocombe a. ., Hughes D., Shaw S. The effect of environment on the fatigue of bonded composite joints. Part 1: testing and fractography. Compos Part A Appl Sci Manuf 2001;32:45–58.
[32] Correia J. Effects of hygrothermal ageing on the mechanical properties of glass-fibre-reinforced polymer pultruded profiles. Struct ... 2010.
[33] Weitsman YJ. Anomalous fluid sorption in polymeric composites and its relation to fluid-induced damage. Compos Part A Appl Sci Manuf 2006;37:617–23.
[34] Karbhari VM, Ghosh K. Comparative durability evaluation of ambient temperature cured externally bonded CFRP and GFRP composite systems for repair of bridges. Compos Part A Appl Sci Manuf 2009;40:1353–63.
[35] Nishizaki I, Meiarashi S. Long-Term Deterioration of GFRP in Water and Moist Environment. J Compos Constr 2002;6:21–7.
[36] Bradley WL, Grant TS. The effect of the moisture absorption on the interfacial strength of polymeric matrix composites. J Mater Sci 1995;30:5537–42.
[37] Jackson SP, Weitsman Y. Moisture effects and moisture induced damage in composites. Fifth Int. Conf. Compos. Mater. ICCM-V, San Diego, 1985, p. 1435–52.
[38] Helbling CS, Karbhari VM. Investigation of the Sorption and Tensile Response of Pultruded E-Glass/Vinylester Composites Subjected to Hygrothermal Exposure and Sustained Strain. J Reinf Plast Compos 2008;27:613–38.
[39] Chu W, Karbhari VM. Effect of Water Sorption on Performance of Pultruded E-Glass/Vinylester Composites. J Mater Civ Eng 2005;17:63–71.
[40] Yang Q, Karbhari VM, Sikorsky C. Durability study of three prefabricated carbon/epoxy composites and their respective epoxy adhesives used for bonding them to concrete. Int. SAMPE Symp. Exhib., vol. 52, 2008.
[41] Sciolti M, Frigione M, Aiello M. Wet lay-up manufactured FRPs for concrete and masonry repair: influence of water on the properties of composites and on their epoxy components. J Compos ... 2010:823–33.
[42] Blaga A. GRP COMPOSITE MATERIALS IN CONSTRUCTION: PROPERTIES, APPLICATIONS AND DURABILITY-nn 1978.
[43] Kumar SB, Sridhar I, Sivashanker S. Influence of humid environment on the performance of high strength structural carbon fiber composites. Mater Sci Eng A 2008;498:174–8.

[44] Scott P, Lees JM. Effects of solution exposure on the combined axial-shear behaviour of unidirectional CFRP rods. Compos Part A Appl Sci Manuf 2012;43:1599–611.
[45] Gibbins MN, Hoffman DJ. Environmental Exposure Effects on Composite Materials for Commercial Aircraft. DTIC Document; 1982.
[46] Joshi OK. The effect of moisture on the shear properties of carbon fibre composites. Composites 1983;14:196–200.
[47] Zhang M, Mason SE. The effects of contamination on the mechanical properties of carbon fibre reinforced epoxy composite materials. J Compos Mater 1999;33:1363–74.
[48] Akepati AR, Nair AR, Roy S, Haque A, Dutta PK, Kumar A. Environmental Degradation of Interlaminar Shear Strength in Carbon/Epoxy Composites. In: Jain R, Lee L, editors. Fiber Reinf. Polym. Compos. Infrastruct. Appl., Dordrecht: Springer Netherlands; 2012.
[49] Goruganthu S, Elwell J, Ramasetty A, Nair AR, Roy S, Haque A, et al. Characterization and modeling of the effect of environmental degradation on interlaminar shear strength of carbon/epoxy composites. Polym Polym Compos 2008;16:165–79.
[50] Choqueuse D, Davies P, Mazéas F, Baizeau R. Aging of composites in water: Comparison of five materials in terms of absorption kinetics and evolution of mechanical properties. ASTM Spec Tech Publ 1997;1302:73–96.
[51] Botelho EC, Pardini LC, Rezende MC. Hygrothermal effects on the shear properties of carbon fiber/epoxy composites. J Mater Sci 2006;41:7111–8.
[52] Cabral-Fonseca S, Nunes JP, Rodrigues MP, Eusébio MI. Durability of carbon fibre reinforced polymer laminates used to reinforced concrete structures. Sci Eng Compos Mater 2011;18.
[53] Liao K, Schultheisz CR, Hunston DL, Brinson LC. Long-term durability of fiber-reinforced polymer-matrix composite materials for infrastructure applications: A review. J Adv Mater 1998;30:3–40.
[54] WOO M, Piggott MR. Water absorption of resins and composites. IV: Water transport in fiber reinforced plastics. J Compos Technol Res 1988;10:20–4.
[55] Park GS, Crank J. Diffusion in polymers 1968.
[56] Chin JW, Nguyen T, Aouadi K. Sorption and diffusion of water, salt water, and concrete pore solution in composite matrices. J Appl Polym Sci 1999;71:483–92.
[57] Weitsman Y, Elahi M. Effects of fluids on the deformation, strength and durability of polymeric composites–an overview. Mech Time-Dependent Mater 2000:107–26.
[58] Carter HG, Kibler KG. Langmuir-Type Model for Anomalous Moisture Diffusion In Composite Resins. J Compos Mater 1978;12:118–31.
[59] Jiang X, Kolstein H, Bijlaard FSK. Moisture diffusion and hygrothermal aging in pultruded fibre reinforced polymer composites of bridge decks. Mater Des 2012;37:304–12.
[60] Jiang X, Kolstein H, Bijlaard F, Qiang X. Effects of hygrothermal aging on glass-fibre reinforced polymer laminates and adhesive of FRP composite bridge: Moisture diffusion characteristics. Compos Part A Appl Sci Manuf 2013;57:49–58.
[61] Vaddadi P, Nakamura T, Singh RP. Inverse Analysis to Determine Hygrothermal Properties in Fiber Reinforced Composites. J Compos Mater 2006;41:309–34.
[62] Ghorbel I, Valentin D. Hydrothermal effects on the physico-chemical properties of pure and glass fiber reinforced polyester and vinylester resins. Polym Compos 1993;14:324–34.
[63] Radha JC, Ranganathaiah C. Effect of the fiber orientation on the sorption kinetics of seawater in an epoxy/glass composite: A free-volume microprobe study. J Appl Polym Sci 2008;109:1302–9.
[64] Pierron F, Poirette Y, Vautrin A. A Novel Procedure for Identification of 3D Moisture Diffusion Parameters on Thick Composites: Theory, Validation and Experimental Results. J Compos Mater 2002;36:2219–43.

[65] Thomason J. The interface region in glass fibre-reinforced epoxy resin composites: 2. Water absorption, voids and the interface. Composites 1995;26:477–85.
[66] Zhang a Y, Zhang DX. Effect of Voids on the Tensile Property of CFRP in Hygrothermal Environment. Adv Mater Res 2012;482-484:1176–9.
[67] Robert M, Roy R, Benmokrane B. Environmental effects on glass fiber reinforced polypropylene thermoplastic composite laminate for structural applications. Polym Compos 2009:NA – NA.
[68] Lagrange A, Melennec C, Jacquemet R. Influence of various stress conditions of the moisture diffusion of composites in distilled water and in natural sea-water. Durab. Polym. based Compos. Syst. Struct. Appl., Springer; 1991, p. 385–92.
[69] Davies P, Mazéas F, Casari P. Sea Water Aging ofGlass Reinforced Composites:Shear Behaviour andDamage Modelling. J Compos Mater 2001;35:1343–72.
[70] Kootsookos a., Mouritz AP. Seawater durability of glass- and carbon-polymer composites. Compos Sci Technol 2004;64:1503–11.
[71] Zhu H-G, Leung CKY, Kim J-K. Durability of GFRP composite made of epoxy/organoclay nanocomposite. Concr Repair, Rehabil Retrofit II 2009:423.
[72] Zhu H-G, Leung CK, Kim J-K, Liu M-Y. Tensile properties degradation of GFRP composites containing nanoclay in three different environments. J Compos Mater 2011;46:2179–92.
[73] Hackman I, Hollaway L. Epoxy-layered silicate nanocomposites in civil engineering. Compos Part A Appl Sci Manuf 2006;37:1161–70.
[74] Robert M, Cousin P, Fam A, Benmokrane B. Effect of the addition of modified mica on mechanical and durability properties of FRP composite materials for civil engineering. Polym Compos 2011;32:1202–9.
[75] Gude MR, Prolongo SG, Ureña a. Hygrothermal ageing of adhesive joints with nanoreinforced adhesives and different surface treatments of carbon fibre/epoxy substrates. Int J Adhes Adhes 2013;40:179–87.
[76] Karbhari VM, Project SSR, University of California SDD of SE. Durability Data for FRP Rehabilitation Systems. Department of Structural Engineering, University of California, San Diego; 2009.
[77] Mays GC, Hutchinson AR. Adhesives in civil engineering. Cambridge University Press; 2005.
[78] Tai RCL, Szklarska-Smialowska Z. Effect of fillers on the degradation of automotive epoxy adhesives in aqueous solutions. J Mater Sci 1993;28:6199–204.
[79] Soles CL, Yee AF. A discussion of the molecular mechanisms of moisture transport in epoxy resins. J Polym Sci Part B Polym Phys 2000;38:792–802.
[80] Soles CL, Chang FT, Gidley DW, Yee AF. Contributions of the nanovoid structure to the kinetics of moisture transport in epoxy resins. J Polym Sci Part B Polym Phys 2000;38:776–91.
[81] Rider AN, Brack N, Andres S, Pigram PJ. The influence of hydroxyl group concentration on epoxy–aluminium bond durability. J Adhes Sci Technol 2004;18:1123–52.
[82] Calvez P, Bistac S, Brogly M, Richard J, Verchère D. Mechanisms of interfacial degradation of epoxy adhesive/galvanized steel assemblies: relevance to durability. J Adhes 2012;88:145–70.
[83] Frigione M, Lettieri M, Mecchi AM. Environmental Effects on Epoxy Adhesives Employed for Restoration of Historical Buildings1. J Mater Civ Eng 2006;18:715–22.
[84] Frigione M, Naddeo C, Acierno D. Cold-curing epoxy resins: Aging and environmental effects. I-Thermal properties. J Polym Eng 2001;21:23–52.
[85] Adams RD. Structural adhesive joints in engineering. Springer; 1997.
[86] Adamson MJ. Thermal expansion and swelling of cured epoxy resin used in graphite/epoxy composite materials. J Mater Sci 1980;15:1736–45.

[87] Adams RD, Cowap JW, Farquharson G, Margary GM, Vaughn D. The relative merits of the Boeing wedge test and the double cantilever beam test for assessing the durability of adhesively bonded joints, with particular reference to the use of fracture mechanics. Int J Adhes Adhes 2009;29:609–20.
[88] Albrecht P, Mecklenburg MF. Predicting cohesive strength of a bonded joint from properties of bulk adhesive. First Int. Conf. Compos. Infrastruct., 1996.
[89] Nguyen T-C, Bai Y, Zhao X-L, Al-Mahaidi R. Durability of steel/CFRP double strap joints exposed to sea water, cyclic temperature and humidity. Compos Struct 2012;94:1834–45.
[90] Dawood M, Rizkalla S. Environmental durability of a CFRP system for strengthening steel structures. Constr Build Mater 2010;24:1682–9.
[91] Ashcroft IA, Wahab MM, Crocombe AD, Hughes DJ, Shaw SJ. The effect of environment on the fatigue of bonded composite joints. Part 1: testing and fractography. Compos Part A Appl Sci Manuf 2001;32:45–58.
[92] Abdel Wahab MM, Crocombe a. D, Beevers a., Ebtehaj K. Coupled stress-diffusion analysis for durability study in adhesively bonded joints. Int J Adhes Adhes 2002;22:61–73.
[93] Hand HM, Arah CO, McNamara DK, Mecklenburg MF. Effects of environmental exposure on adhesively bonded joints. Constr Build Mater 1992;6:227–34.
[94] Leger R, Roy a., Grandidier JC. A study of the impact of humid aging on the strength of industrial adhesive joints. Int J Adhes Adhes 2013;44:66–77.
[95] Sugiman S, Crocombe a. D, Aschroft I a. Experimental and numerical investigation of the static response of environmentally aged adhesively bonded joints. Int J Adhes Adhes 2013;40:224–37.
[96] Lettieri M, Frigione M. Effects of humid environment on thermal and mechanical properties of a cold-curing structural epoxy adhesive. Constr Build Mater 2012;30:753–60.
[97] Lapique F, Redford K. Curing effects on viscosity and mechanical properties of a commercial epoxy resin adhesive. Int J Adhes Adhes 2002;22:337–46.
[98] Bordes M, Davies P, Cognard J-Y, Sohier L, Sauvant-Moynot V, Galy J. Prediction of long term strength of adhesively bonded steel/epoxy joints in sea water. Int J Adhes Adhes 2009;29:595–608.
[99] Lin YC, Chen X. Moisture sorption–desorption–resorption characteristics and its effect on the mechanical behavior of the epoxy system. Polymer (Guildf) 2005;46:11994–2003.
[100] Roy A, Gontcharova-Benard E, Gacougnolle JL, Davies P. Hygrothermal effects on failure mechanisms of composite/steel bonded joints. ASTM Spec Tech Publ 2000;1357:353–71.
[101] Kinloch AJ. The science of adhesion. J Mater Sci 1982;17:617–51.
[102] Liljedahl CDM, Crocombe a. D, Wahab M a., Ashcroft I a. Modelling the environmental degradation of adhesively bonded aluminium and composite joints using a CZM approach. Int J Adhes Adhes 2007;27:505–18.
[103] Johnson WS, Butkus LM. Considering environmental conditions in the design of bonded structures: A fracture mechanics approach. Fatigue Fract Eng Mater Struct 1998;21:465–78.
[104] Loh WK, Crocombe AD, Wahab MMA, Watts JF, Ashcroft IA. The effect of moisture on the failure locus and fracture energy of an epoxy–steel interface. J Adhes Sci Technol 2002;16:1407–29.
[105] Da Silva LFM, Dillard DA, Blackman B, Adams RD. Testing adhesive joints: best practices. John Wiley & Sons; 2013.
[106] Ameli A, Datla N V, Papini M, Spelt JK. Hygrothermal properties of highly toughened epoxy adhesives. J Adhes 2010;86:698–725.
[107] Datla NV, Ameli a., Azari S, Papini M, Spelt JK. Effects of hygrothermal aging on the fatigue behavior of two toughened epoxy adhesives. Eng Fract Mech 2012;79:61–77.

[108] Loh WK, Crocombe a. D, Abdel Wahab MM, Ashcroft I a. Modelling anomalous moisture uptake, swelling and thermal characteristics of a rubber toughened epoxy adhesive. Int J Adhes Adhes 2005;25:1–12.
[109] Vanlandingham MR, Eduljee RF, Gillespie JW. Moisture diffusion in epoxy systems. J Appl Polym Sci 1999;71:787–98.
[110] Mubashar a., Ashcroft I a., Critchlow GW, Crocombe a. D. Moisture absorption–desorption effects in adhesive joints. Int J Adhes Adhes 2009;29:751–60.
[111] Al-Harthi M, Loughlin K, Kahraman R. Moisture diffusion into epoxy adhesive: testing and modeling. Adsorption 2007;13:115–20.
[112] Glaskova TI, Guedes RM, Morais JJ, Aniskevich AN. A comparative analysis of moisture transport models as applied to an epoxy binder. Mech Compos Mater 2007;43:377–88.
[113] Scott P, Lees JM. Water, salt water, and alkaline solution uptake in epoxy thin films. J Appl Polym Sci 2013;130:1898–908.
[114] Mubashar A, Ashcroft IA, Critchlow GW, Crocombe AD. Modelling cyclic moisture uptake in an epoxy adhesive. J Adhes 2009;85:711–35.
[115] Kahraman R, Al-Harthi M. Moisture diffusion into aluminum powder-filled epoxy adhesive in sodium chloride solutions. Int J Adhes Adhes 2005;25:337–41.
[116] Zanni-Deffarges MP, Shanahan MER. Diffusion of water into an epoxy adhesive: comparison between bulk behaviour and adhesive joints. Int J Adhes Adhes 1995;15:137–42.
[117] Linossier I, Gaillard F, Romand M, Nguyen T. A Spectroscopic Technique for Studies of WaterTransport Along the Interface and Hydrolytic Stability of Polymer/Substrate Systems. J Adhes 1999;70:221–39.
[118] Wapner K, Grundmeier G. Spatially resolved measurements of the diffusion of water in a model adhesive/silicon lap joint using FTIR-transmission-microscopy. Int J Adhes Adhes 2004;24:193–200.
[119] O'Brien EP, Reboa PF, Field M, Pullen D, Markel D, Ward TC. A novel impedance sensor design for measuring the distribution and transport of fluids at the interface. Int J Adhes Adhes 2003;23:335–8.
[120] Liljedahl CDM, Crocombe a. D, Gauntlett FE, Rihawy MS, Clough a. S. Characterising moisture ingress in adhesively bonded joints using nuclear reaction analysis. Int J Adhes Adhes 2009;29:356–60.
[121] Davis GD, Pethrick RA, Doyle J. Detection of Moisture in Adhesive Bonds Using Electrochemical Impedance and Dielectric Spectroscopies. J Adhes Sci Technol 2009;23:507–28.
[122] Chauffaille S, Devos O, Jumel J, Shanahan MER. Liquid diffusion in polymeric adhesives by electrochemical-impedance spectroscopy (EIS). Int J Adhes Adhes 2010;30:602–8.
[123] Adams RD. Adhesive bonding: science, technology and applications. CRC Press Cambridge; 2005.
[124] Posner R, Ozcan O, Grundmeier G. Water and ions at polymer/metal interfaces. Des. Adhes. Joints Under Humid Cond., Springer; 2013, p. 21–52.
[125] Hua Y, Crocombe AD, Wahab MA, Ashcroft IA. Modelling Environmental Degradation in EA9321-Bonded Joints using a Progressive Damage Failure Model. J Adhes 2006;82:135–60.
[126] Hutchinson AR, Hollaway LC. Environmental durability. Strength Reinf Concr Struct Using Externally-Bonded Frp Compos Struct Civ Eng 1999:156.
[127] Oudad W, Madani K, Bachir Bouiadjra B, Belhouari M, Cohendoz S, Touzain S, et al. Effect of humidity absorption by the adhesive on the performances of bonded composite repairs in aircraft structures. Compos Part B Eng 2012;43:3419–24.
[128] Mcgeorge D. On the Long Term Properties of Steel- Composite Interfaces for Marine Applications 2005.

[129] Aiello MA, Frigione M, Acierno D. Effects of Environmental Conditions on Performance of Polymeric Adhesives for Restoration of Concrete Structures. J Mater Civ Eng 2002;14:185–9.
[130] Stratford TJ, Bisby LA. Effect of Warm Temperatures on Externally Bonded FRP Strengthening. J Compos Constr 2012;16:235–44.
[131] ASTM International. D5229/D5229M-14. Standard Test Method for Moisture Absorption Properties and Equilibrium Conditioning of Polymer Matrix Composite Materials 2014.
[132] ASTM International. D638 - 10. Standard Test Method for Tensile Properties of Plastics 2010.
[133] Michels J, Sena-Cruz J, Czaderski C, Motavalli M. Structural Strengthening with Prestressed CFRP Strips with Gradient Anchorage. J Compos Constr 2013;17:651–61.
[134] ASTM International. D3039/D3039M - 14. Standard test method for tensile properties of polymer matrix composite materials. Annu B ASTM Stand 2014:1–13.
[135] André A, Haghani R, Biel A. Application of fracture mechanics to predict the failure load of adhesive joints used to bond CFRP laminates to steel members. Constr Build Mater 2012;27:331–40.
[136] Salimi S. Application of cohesive modeling in joining technology: Thick adhesive layers and rivet joints. University of Skövde, 2012.
[137] Ameli a., Papini M, Spelt JK. Fracture R-curve of a toughened epoxy adhesive as a function of irreversible degradation. Mater Sci Eng A 2010;527:5105–14.
[138] Zhang Y. Fracture and Fatigue of Adhesively-Bonded Fiber-Reinforced Polymer Structural Joints. EPFL, 2010.
[139] De Moura M, Dourado N. Mode II fracture characterization of bonded joints using the ELS test. Test. Adhes. Joints Best Pract., Wiley-VCH; 2013, p. 186–91.
[140] Haghani R, Al-Emrani M. A new design model for adhesive joints used to bond FRP laminates to steel beams. Constr Build Mater 2012;30:686–94.
[141] Stigh U, Alfredsson KS, Andersson T, Biel A, Carlberger T, Salomonsson K. Some aspects of cohesive models and modelling with special application to strength of adhesive layers. Int J Fract 2010;165:149–62.
[142] Barenblatt G. Equilibrium cracks formed during brittle fracture rectilinear cracks in plane plates. J Appl Math Mech 1959.
[143] Barenblatt G. The mathematical theory of equilibrium cracks in brittle fracture. Adv Appl Mech 1962;7:55–129.
[144] Sugiman S, Crocombe a. D, Aschroft I a. Modelling the static response of unaged adhesively bonded structures. Eng Fract Mech 2013;98:296–314.
[145] Gustafson P a., Waas AM. The influence of adhesive constitutive parameters in cohesive zone finite element models of adhesively bonded joints. Int J Solids Struct 2009;46:2201–15.
[146] Katnam KB, Crocombe a. D, Sugiman H, Khoramishad H, Ashcroft I a. Static and Fatigue Failures of Adhesively Bonded Laminate Joints in Moist Environments. Int J Damage Mech 2011;20:1217–42.
[147] Lee D-B, Ikeda T, Miyazaki N, Choi N-S. Effect of Bond Thickness on the Fracture Toughness of Adhesive Joints. J Eng Mater Technol 2004;126:14.